Supplementary Figures

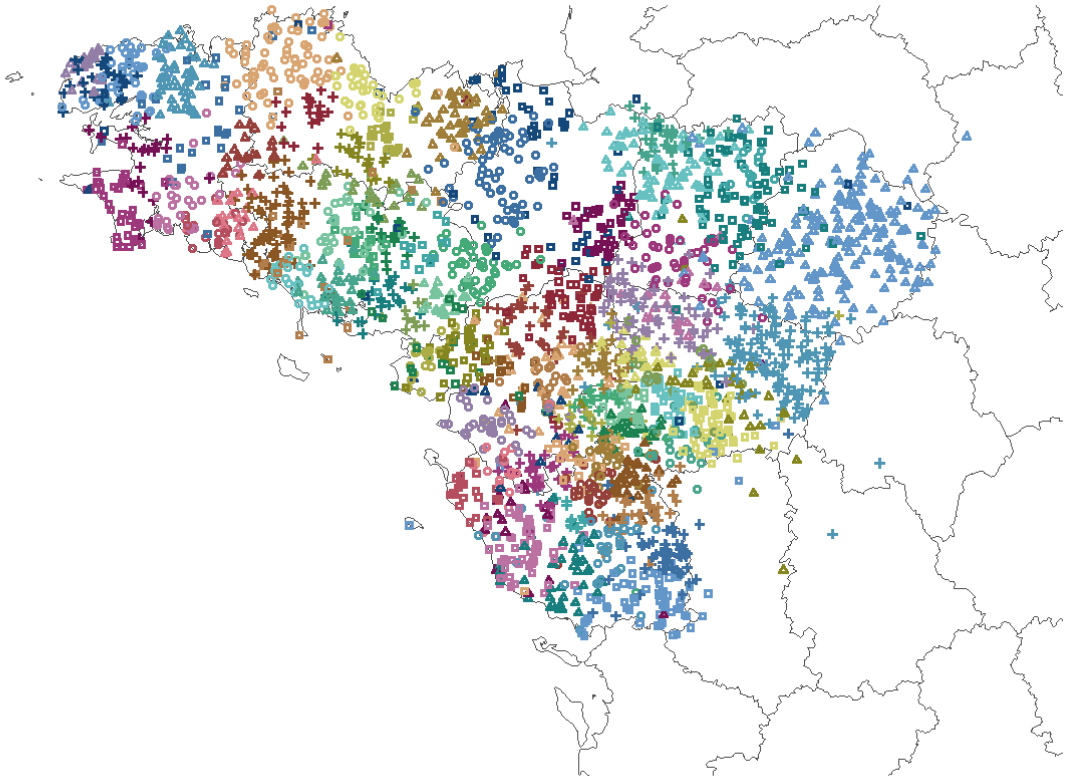

Figure S1. fineSTRUCTURE results for k=154. But only clusters with >10 individuals (78 clusters) are shown. Map generated with *R statistical package* using *sp* package and the "*départements"* boundary dataset from the French platform of open data (https://www.data.gouv.fr/).

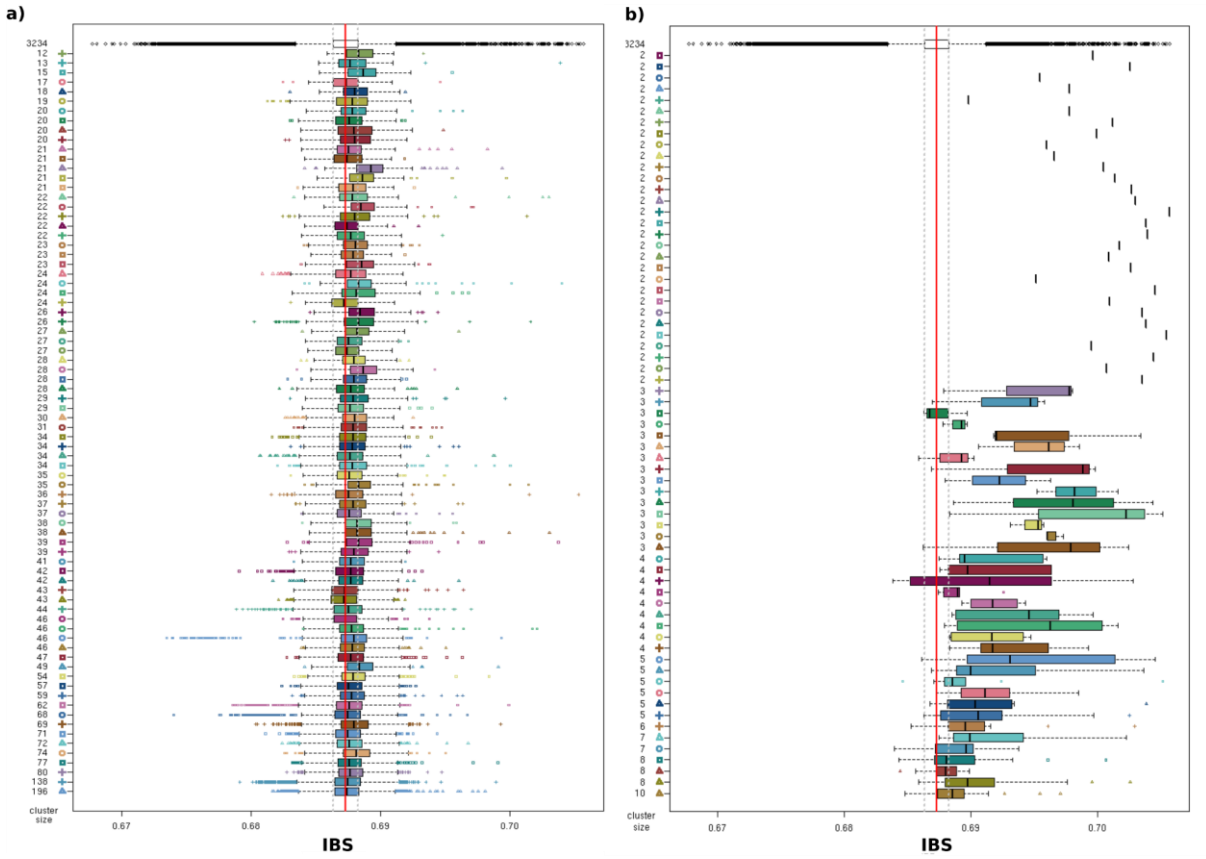

Figure S2. Identity-by-state (IBS) distances computed between pairs of individuals within the 154 clusters for the finest level of population structure. The white box plot represents the distribution of pairwise IBS values, computed with plink *--genome* option, across the whole dataset. Pairwise IBS values are shown in the x-axis while the y-axis shows the 78 clusters with n > 10 (a) and the remaining clusters with n <= 10 (b). Boxplots are coloured according to the cluster colours in Fig. S1. The distributions of relatedness, here captured by the IBS distances, within clusters globally match that computed across the whole sample (median distribution within the 25th-75th percentiles). This occurs for most clusters with a n>10 (a). However, a departure from the whole distribution is observed for many of the clusters with a n < 10 (b). Given that fineSTRUCTURE detects groups of individuals with higher identity-by-descent, the smaller groups with increased IBS likely represent very recent shared ancestry (e.g., family relationships undetectable in the questionnaire, inbreeding).

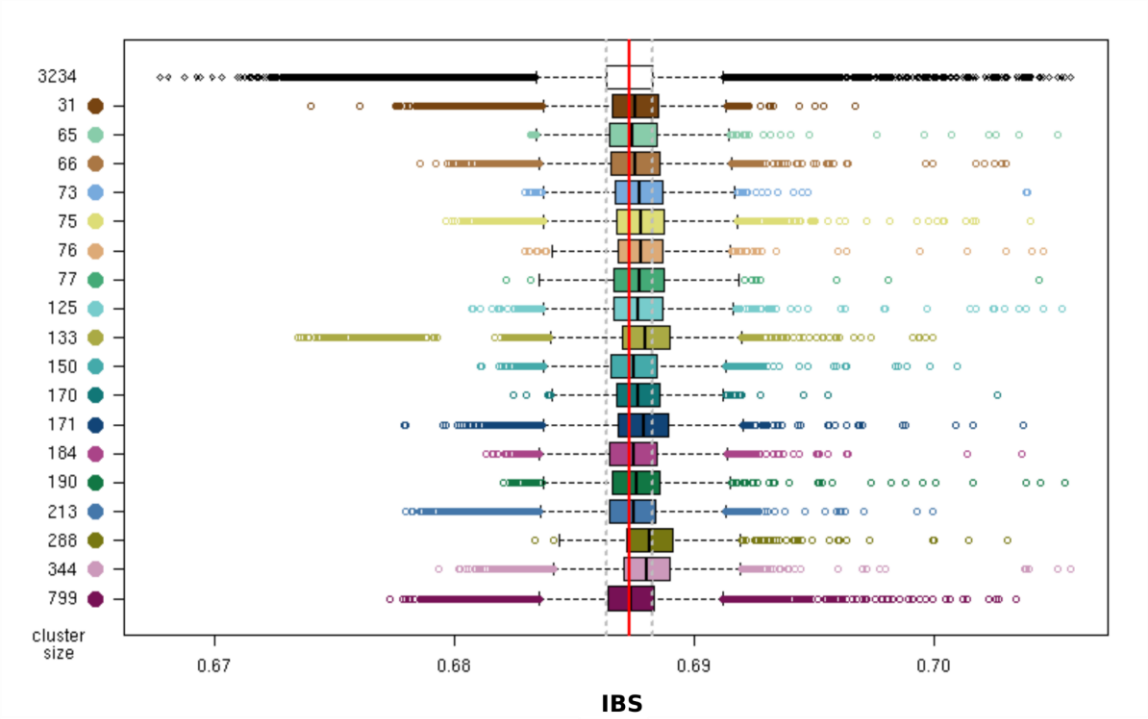

Figure S3. Identity-by-state (IBS) between pairs of individuals belonging to the 18 clusters inferred based on the TVD-based tree on fineSTRUCTURE clustering results. The distributions of relatedness within the 18 clusters (discussed in the main text) match that computed across the whole sample (white boxplot), indicating that individuals within clusters (n > 10) do not exhibit significantly more IBS than pairs of randomly selected individuals in the whole sample. Nevertheless, relatedness distributions slightly shift towards higher values as expected given that population structure is caused by shared ancestry. Such shared ancestry should be reflected over a large timescale and not only restricted to very recent periods (IBS ~ 1). Boxplots are coloured according to the cluster colours in Fig. 1d (main text).

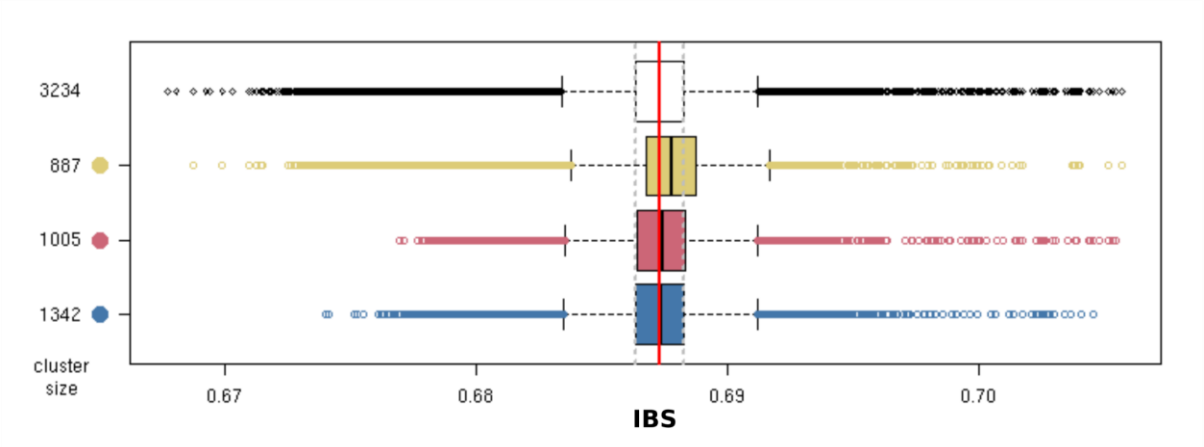

Figure S4. Identity-by-state (IBS) between pairs of individuals within the three clusters. The distributions of relatedness within the three clusters (Fig. 1a) match those computed across the whole sample (white boxplot), indicating that individuals within clusters (n > 10) do not exhibit significantly more IBS than pairs of randomly selected individuals in the whole sample. Overall, we conclude that fine-scale structure found in our study is not due to an overrepresentation of recently related samples.

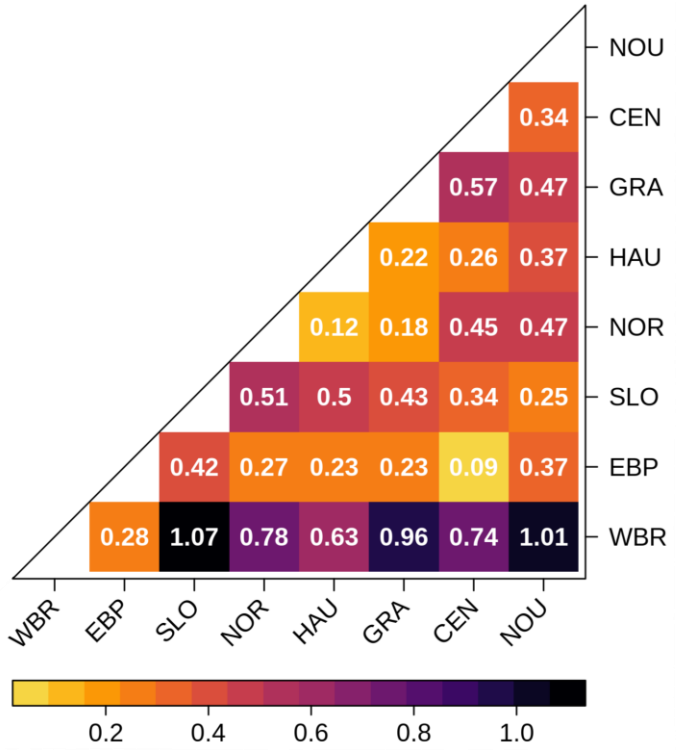

Figure S5. Pairwise average Weir and Cockerham's F_{ST}s within France x 1000**.** F_{ST} values were computed on the WGS dataset after pruning for LD and using n=25 samples/population with the exception of Normandy whose n=19. Cluster names: Western Brittany (WBR), Eastern Brittany/*Pays-de-la-Loire* (EBP) and South Loire (SLO). Population acronyme: NOR, *Normandie*; HAU, Hauts-de-France; GRA, Grand Est; CEN, Centre-Val de Loire; NOU, Nouvelle-Aquitaine.

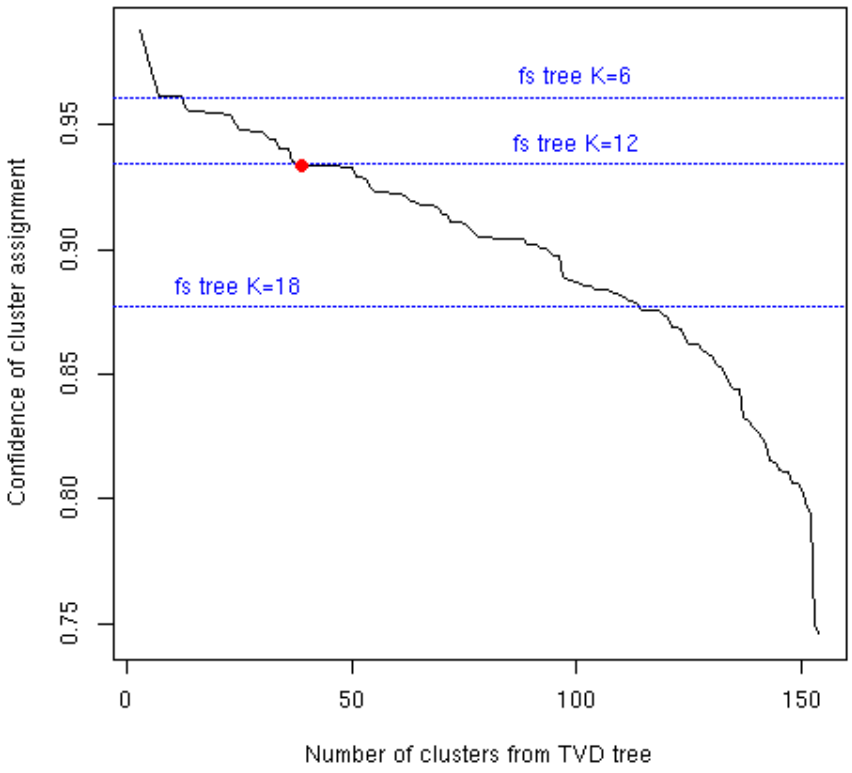

Figure S6. Confidence of cluster assignment from fineSTRUCTURE and TVD-based trees. FS-tree has lower confidence of cluster assignment than TVD-based tree for the same levels of number of clusters. For example, cluster assignment confidence retrieved for k=39 in TVD-based tree (red point) is similar for k=12 in FS-tree. See Material and Methods for details on the computation of cluster confidence (ChromoPainter and fineSTRUCTURE).

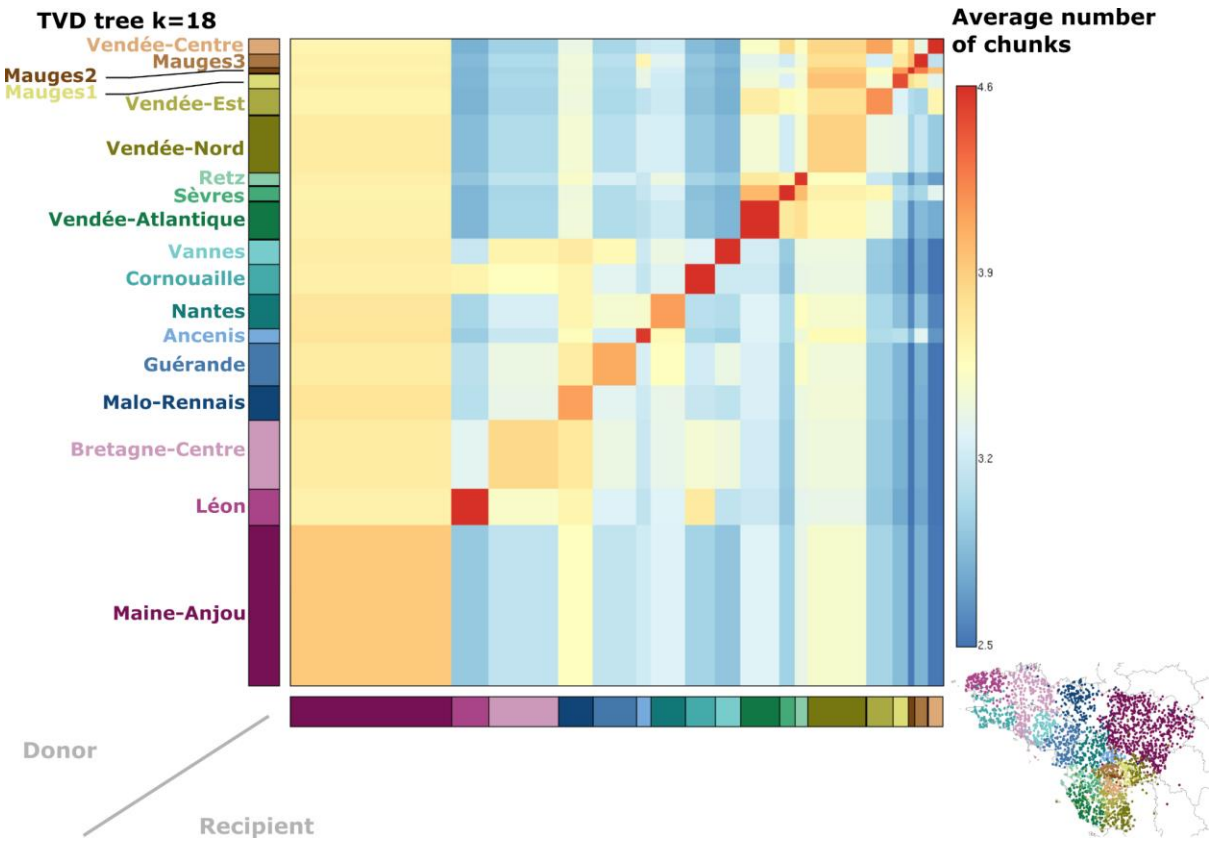

Figure S7. Population-level coancestry matrix for k=18. This matrix was based on the individual-level coancestry (chunkcount matrix) used in cluster inference. Along the columns is shown the average chunk counts a recipient cluster (bottom) received from the donor clusters (on the left) while across the rows is shown the average chunk count that donor clusters (on the left) have contributed to the recipient clusters (bottom). The diagonal represents the average chunk count between pairs of individuals assigned to the same cluster, i.e. the "drift component". In order to visualise the bulk of the variation, only values between 1-99 percentile were considered and those exceeding the range were coloured according to the closer 1 or 99 percentile value. Warmer colours indicate higher levels of ancestry sharing. Map generated in *R statistical package* using *sp* package and the "*départements"* boundary dataset from the French platform of open data (https://www.data.gouv.fr/).

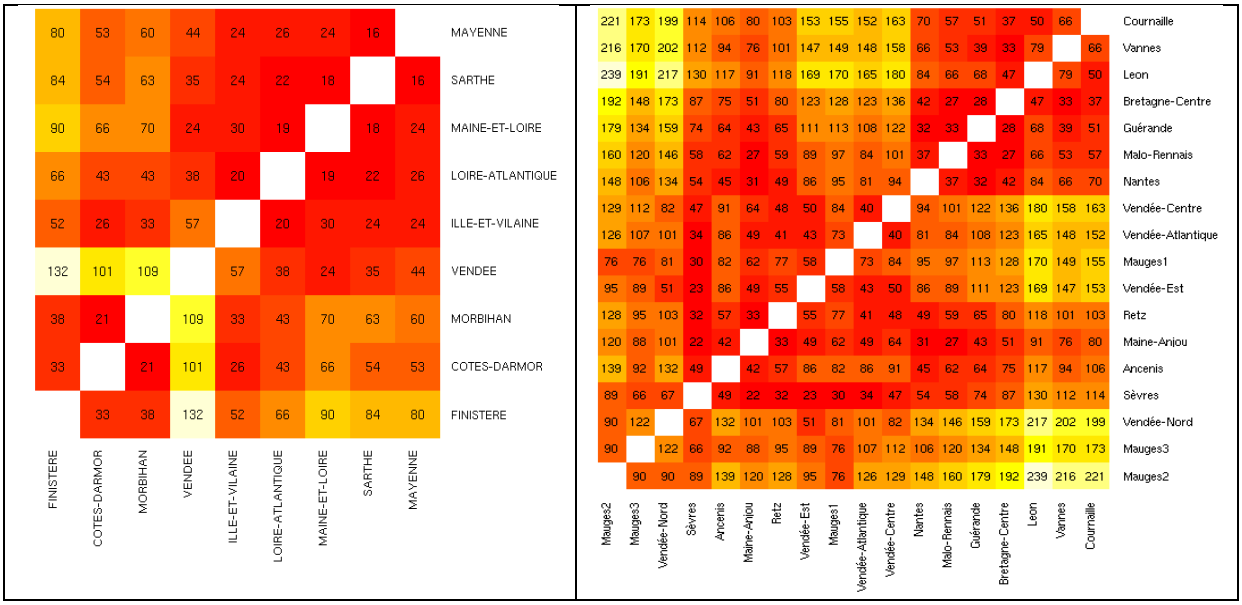

Figure S8. Pairwise F_{ST} values multiplied by 100,000 between the *départements* of Brittany and *Pays-de-la-Loire* (left panel) and the 18 clusters in Northwestern France (right panel) identified in PREGO dataset with fineSTRUCTURE (Fig. 1d, main text)**.**

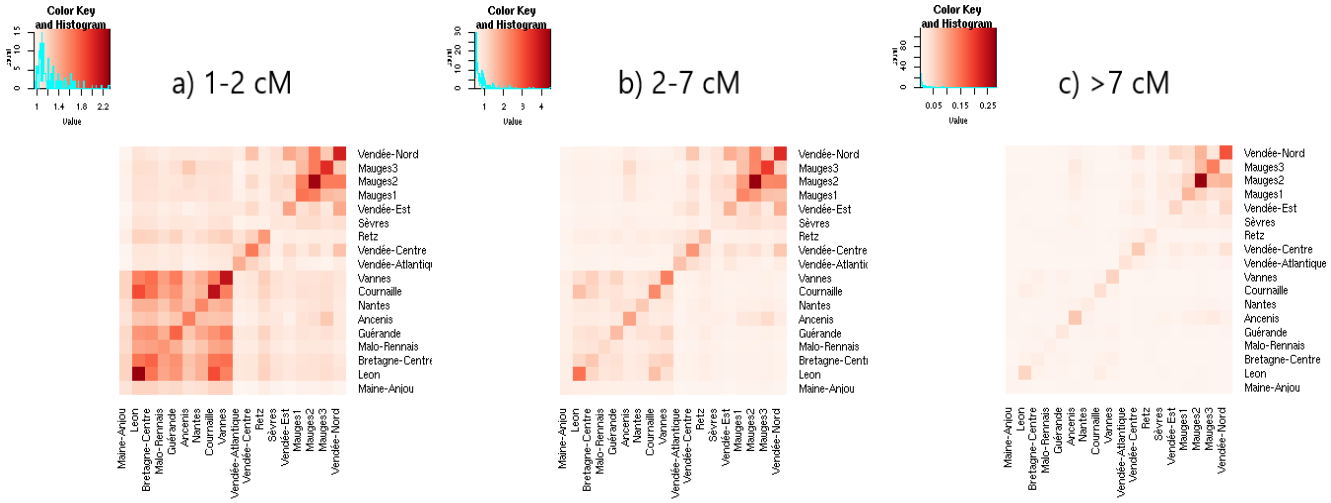

Figure S9. Identity-by-descent (IBD) sharing between pairs of individuals belonging to the 18 clusters identified with the TVD-based tree on fineSTRUCTURE (Fig. 1d main text) results for different chromosome segment sizes (a-c). Segment sizes are indicated over the heatmaps. Heatmap columns (from bottom to up) and rows (left to right) are ordered similarly to the coancestry matrices (see above).

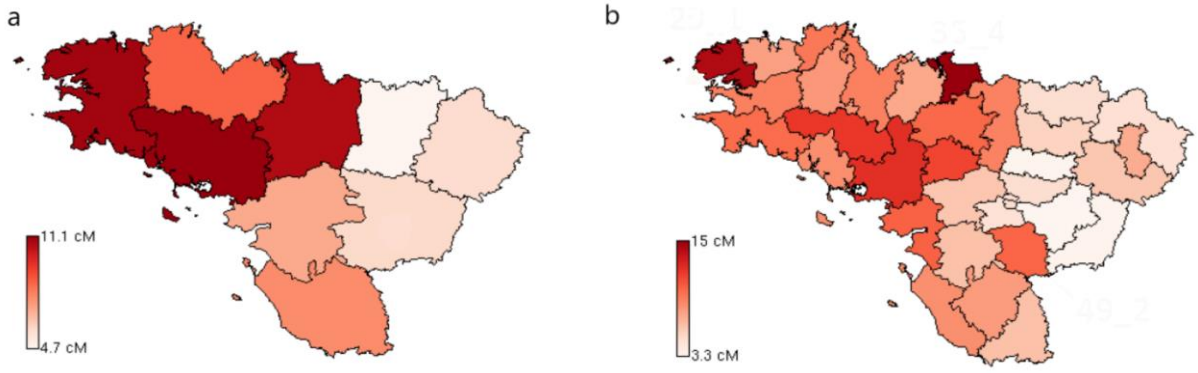

Figure S10. Heatmap displaying average length of runs of homozygosity (ROH) across individuals within a) *départements* and b) *arrondissements* of Northwestern France. The regions of Brittany and Mauges display large ROH indicating smaller effective population sizes Map generated with *R statistical package* using *sp* package and the "***départements***" and "*communes*" boundary dataset from the French platform of open data (https://www.data.gouv.fr/) and OpenStreetMap.

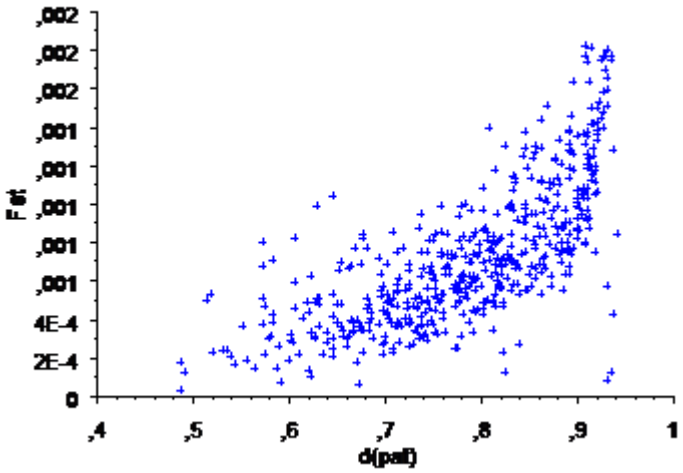

Figure S11. Correlation between surname distance and F_{ST} (negative F_{ST} removed), partial spearman correlation = 0.68.

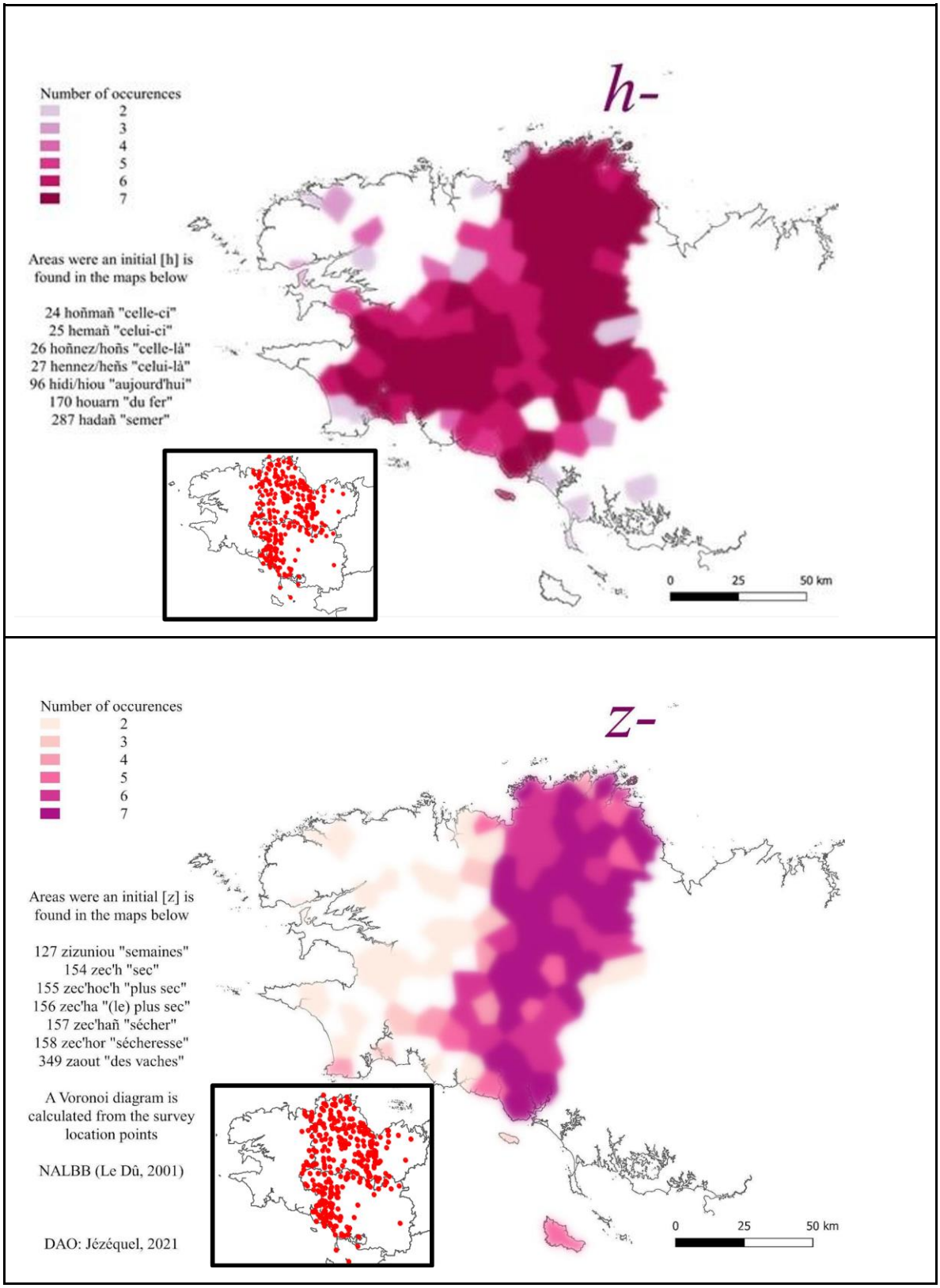

Figure S12. Distribution of the initials h- (upper) and z- (lower) outlining a central dialectal Breton area in Lower Brittany (See Supplementary Discussion). Both linguistic features overlap, at least to some extent, with the distribution of the cluster “Bretagne-Centre” (inset).

The usage of two initial consonants: the aspirated [h] instead of an unaspirated and the alveolar fricative [z] instead of [s], are linguistic features associated with dialectal areas of Breton as described in the *Nouvel Atlas Linguistique de Basse-Bretagne* (Le Dû 2001). The maps were obtained by overlapping word-specific maps of presence/absence across regions. The number of occurrences within polygons were computed using seven words (described on the left) in both cases. For instance, in the case of the occurrences of the initial *h-,* whose pronunciation changes are observed in words like *honman, heman, honnez, hennez, hidi, houarn, hadan,* darker fuchsia polygons mean that these seven words are present therein. Map generated with QGIS 3.22.11 (http://www.qgis.org/). Background map data from Diffusion.shom (https://diffusion.shom.fr/multiproduct/product/configure/id/93) is released under a CC BY-SA 4.0 license (https://creativecommons.org/licenses/by-sa/4.0/). Histolitt® Coastline data ©IGN-Shom 2009.

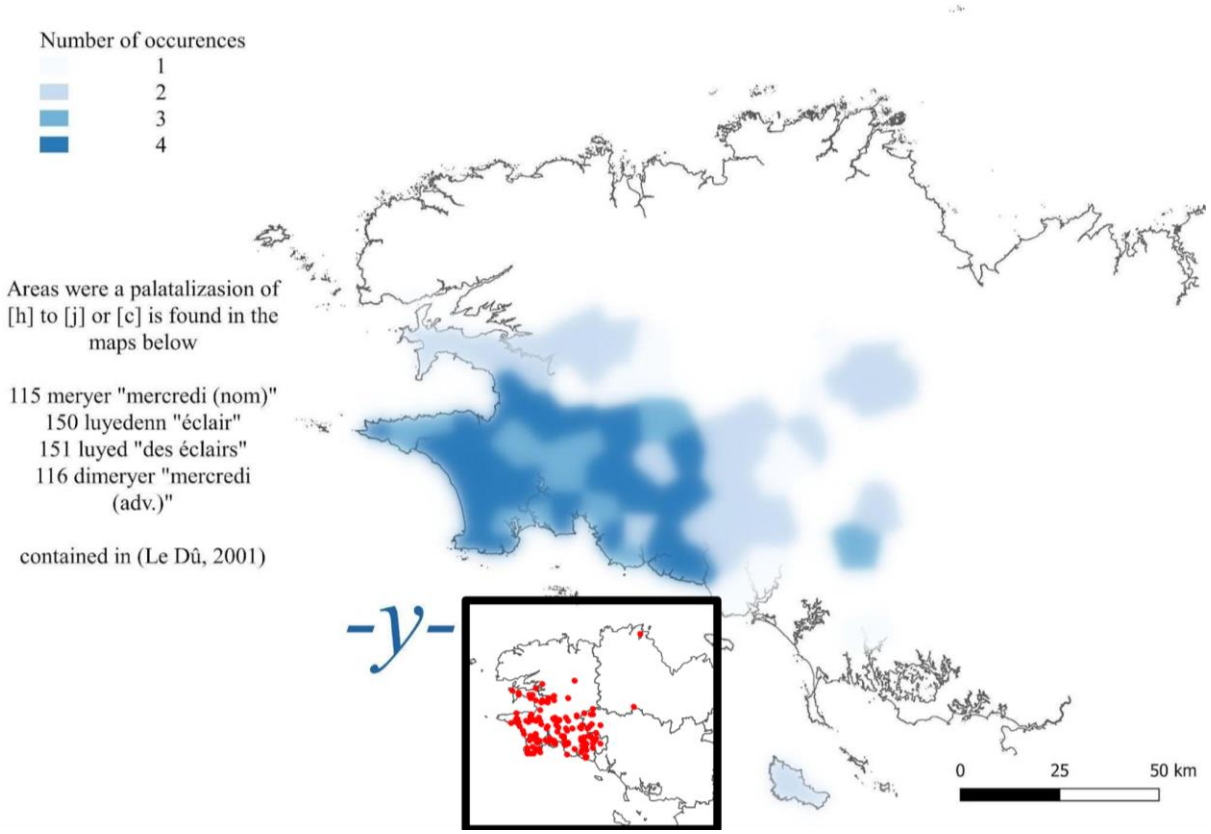

Figure S13. Distribution of the palatalisation of the *-h-* into *-y-* outlining a south-western dialectal area in Lower Brittany (See Supplementary Discussion). This linguistic feature was found to overlap with the distribution of the cluster “Cornouailles” (inset). The map was generated similarly to those in Fig. S12 (above), but focus on four words. Map generated with QGIS 3.22.11 (http://www.qgis.org/). Background map data from Diffusion.shom (https://diffusion.shom.fr/multiproduct/product/configure/id/93) is released under a CC BY-SA 4.0 license (https://creativecommons.org/licenses/by-sa/4.0/). Histolitt® Coastline data ©IGN-Shom 2009.

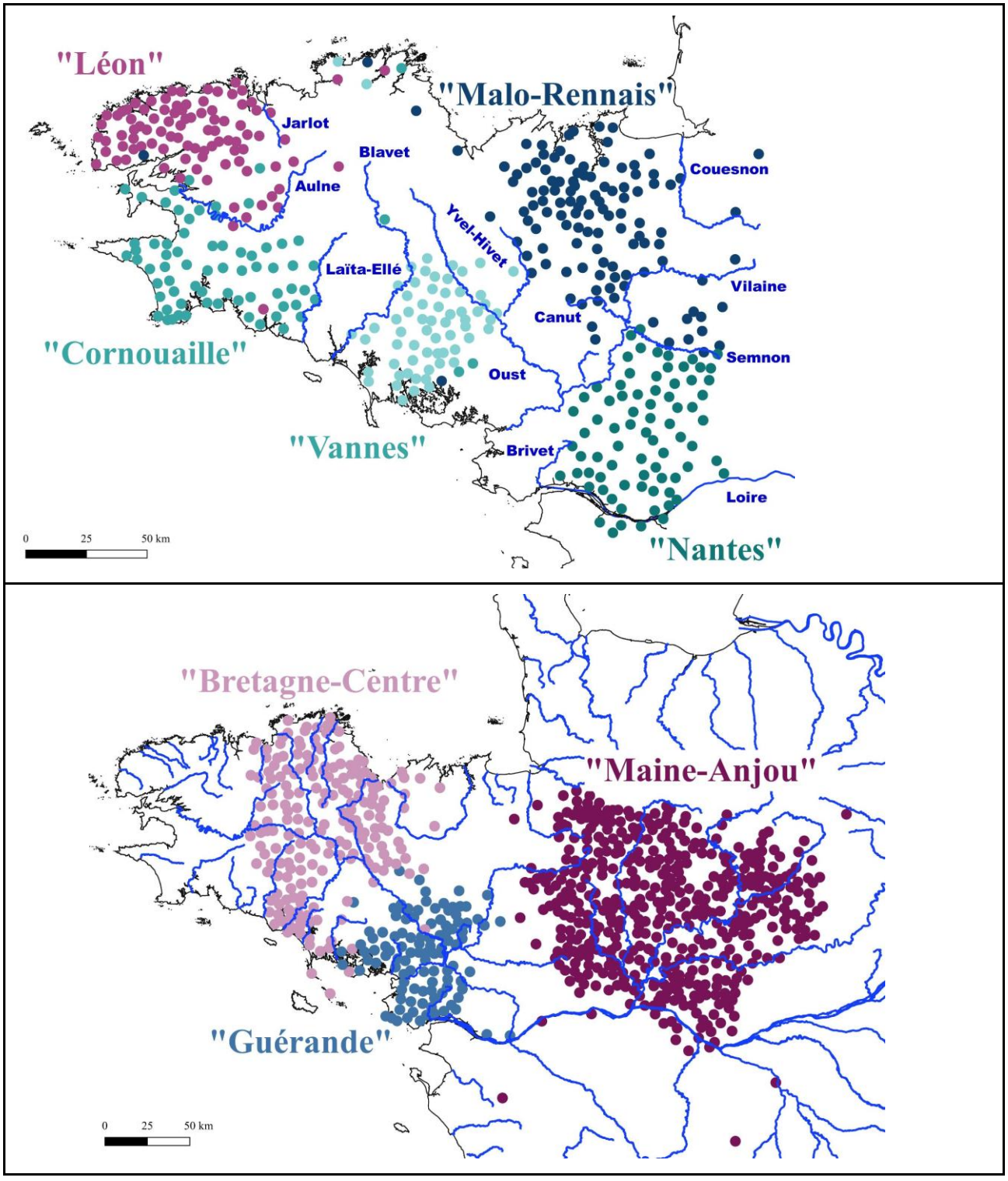
"Léon"
"Malo-Rennais"
Jarlot
Blavet
Aulne
Couesnon
Yvel-Hivet
Laïta-Ellé
Vilaine
Canut
"Cornouaille"
Semnon
Oust
"Vannes"
Brivet
Loire
"Nantes"
0 25 50 km
"Bretagne-Centre"
"Maine-Anjou"
"Guérande"
0 25 50 km

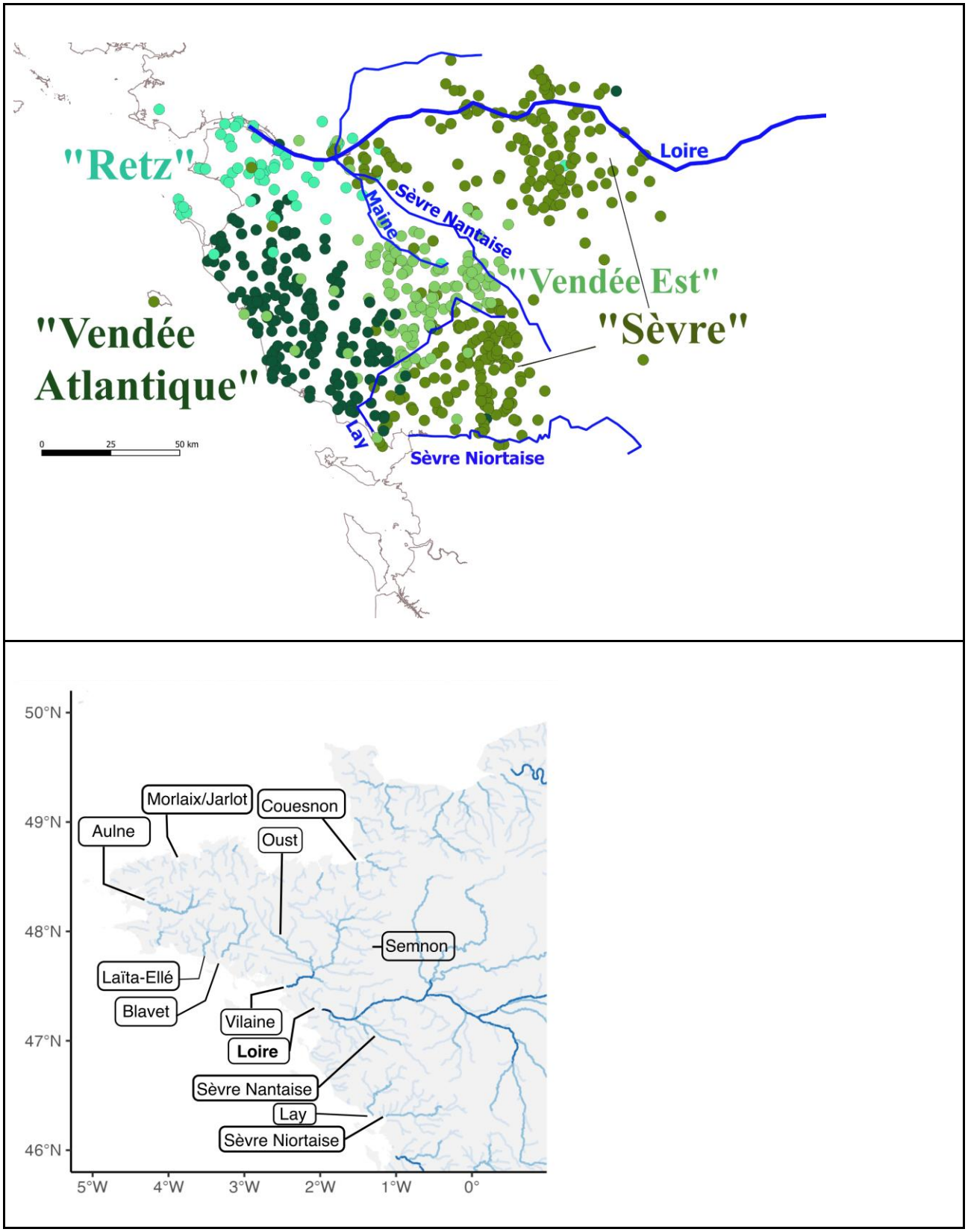

Figure S14. Clusters inferred with fineSTRUCTURE (k=18 of the TVD-tree) and the distribution of local watercourses. The figure is split in three parts and clusters in the Mauges region ("Mauges 1", "Mauges 2" and "Mauges 3") were not displayed to facilitate its visualisation. The first three maps were generated with QGIS 3.22.11 (http://www.qgis.org/). Background map data from Diffusion.shom

(https://diffusion.shom.fr/multiproduct/product/configure/id/93) is released under a CC BY-SA 4.0 license (https://creativecommons.org/licenses/by-sa/4.0/). Histolitt® Coastline data ©IGN-Shom 2009.

The lower map represents the distribution of watercourses (blue) in Northwestern France. The darker the blue the higher the long-term average discharge of the river patch showing that most of the rivers overlapping with the borders of the genetic clusters are the major watercourses. The map was generated using the R statistical package together with the libraries: *ggplot2, sf, dyplr.* Hydrological data was obtained from: https://www.hydrosheds.org.

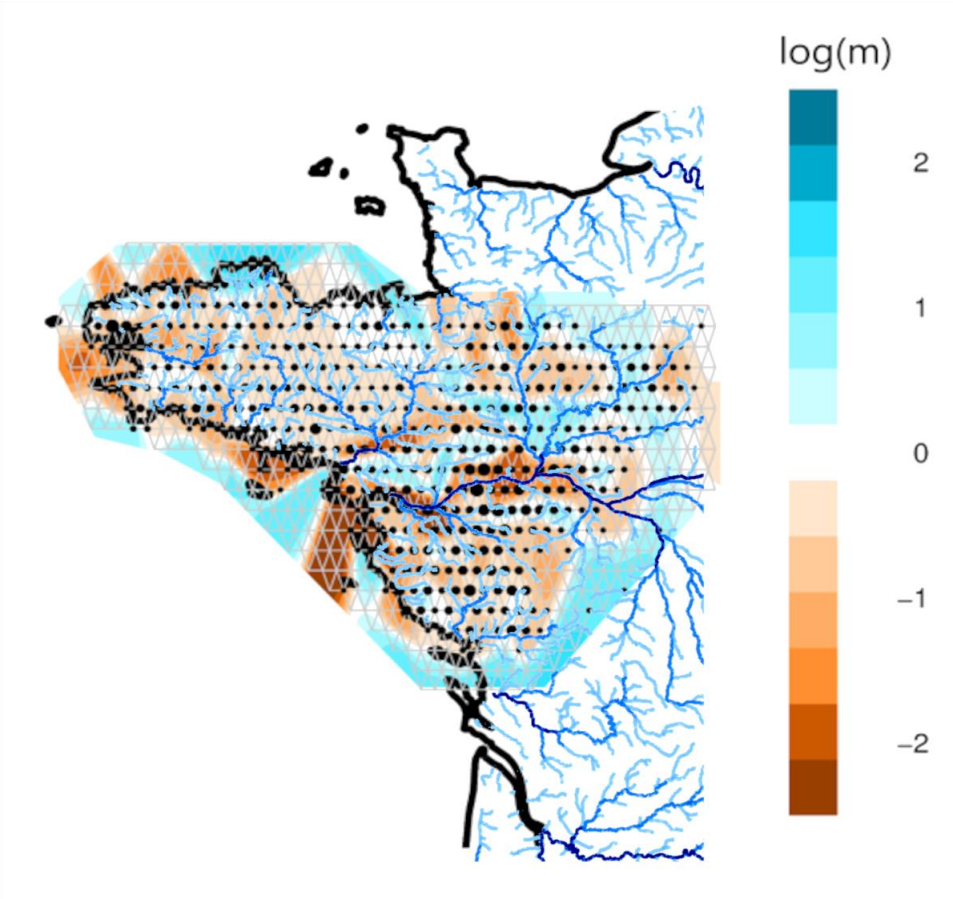

Figure S15. Effective migration surface inferred with EEMS overlapped with geographical location of waterbodies whose colour is proportional to long-term average discharge. Map generated with R statistical package together with the libraries: *ggplot2, sf, dyplr and rEEMSplots.* Hydrological data was obtained from: https://www.hydrosheds.org.

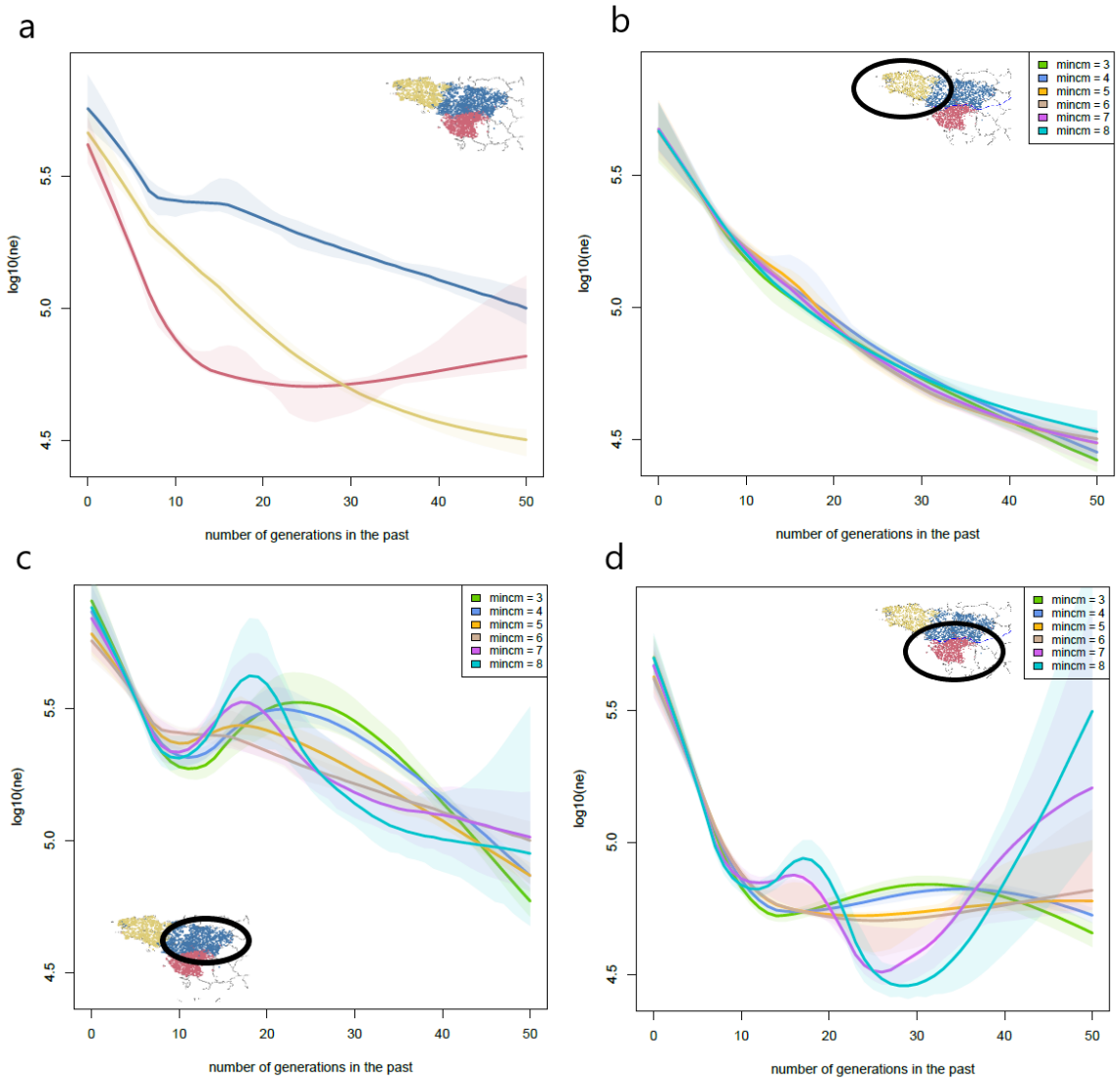

Figure S16. Effective population size trajectories for the three clusters inferred by fineSTRUCTURE (Fig. 1a, main text) obtained with IBDNe. a) IBDNe results for the three clusters together using minimum fragment length (*mincm*) of 6 cM. b-d) IBDNe results for each of the clusters shown in the inset across multiple *mincm* values.

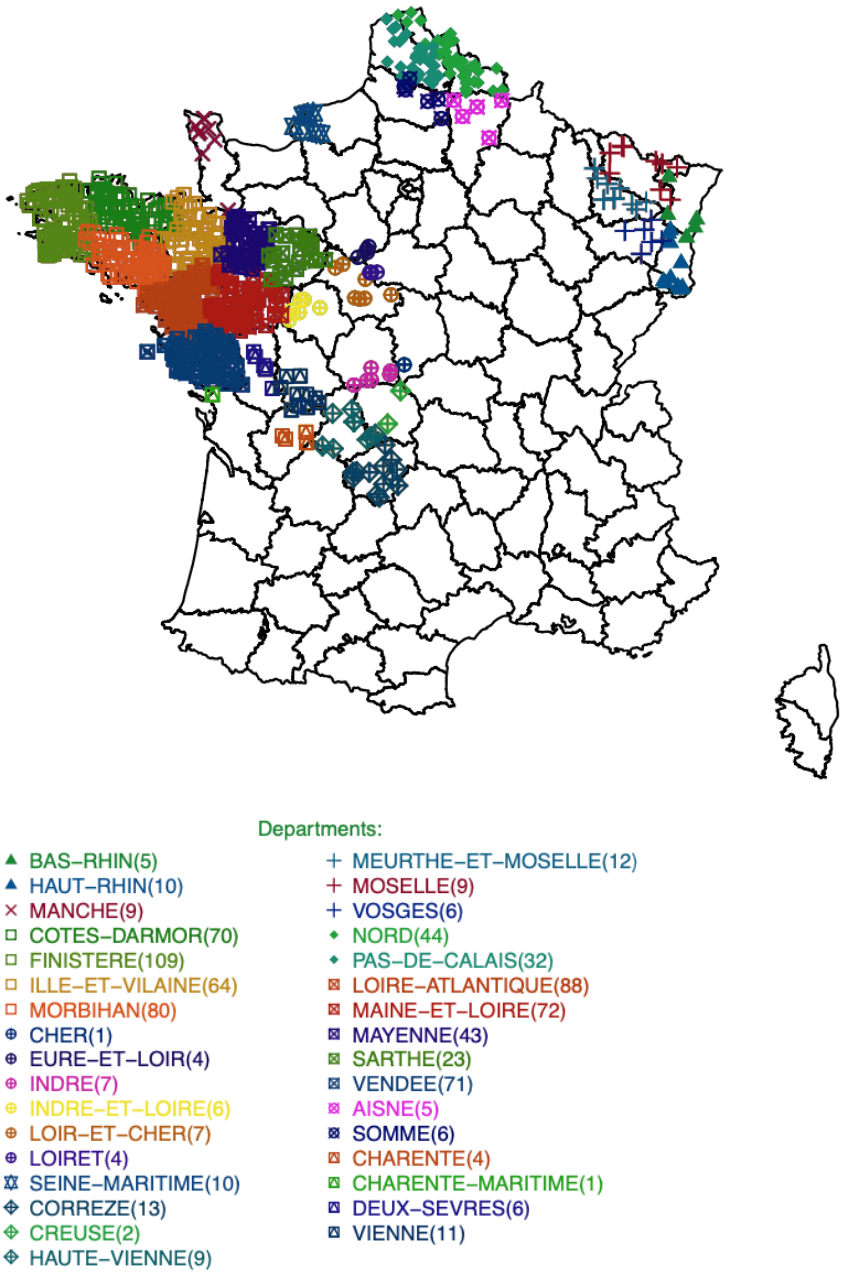

Figure S17. Sample distribution. Out of the 856 samples initially present in the WGS dataset we excluded related samples (PI_HAT > 0.10, three samples) and samples whose four grand-parents were not born in the same *département* (10 samples). The 843 samples are distributed per regions as follows: Brittany (n=323), *Pays-de-la-Loire* (n=297), Normandy (n=19), *Hauts-de-France* (n=87), *Grand Est* (n=42), *Centre* (n=29), *Nouvelle-Aquitaine* (n=46). Map generated with *R statistical package* using *sp* package and the "***départements***" boundary dataset from the French platform of open data (https://www.data.gouv.fr/).

MAC 2	MAC 3-10
k=2	
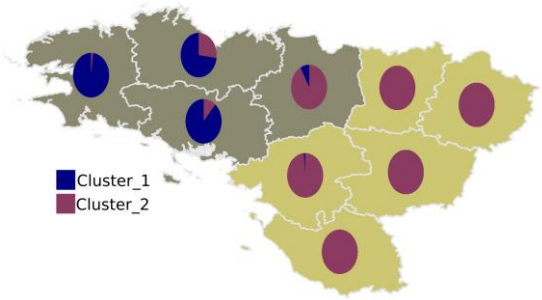	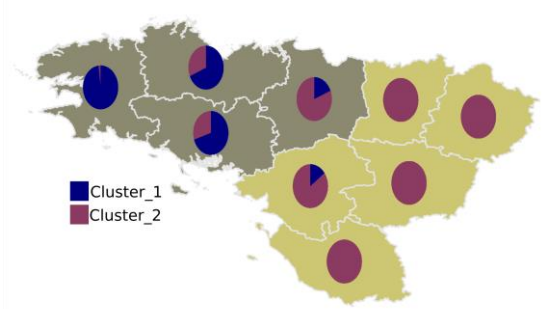
k=5	
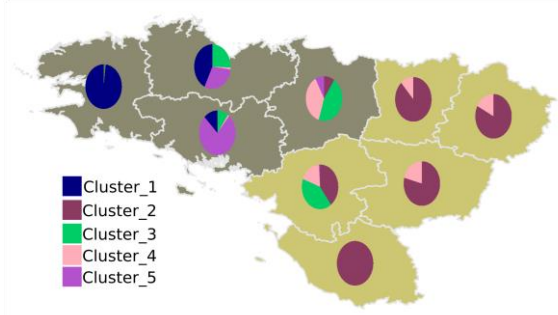	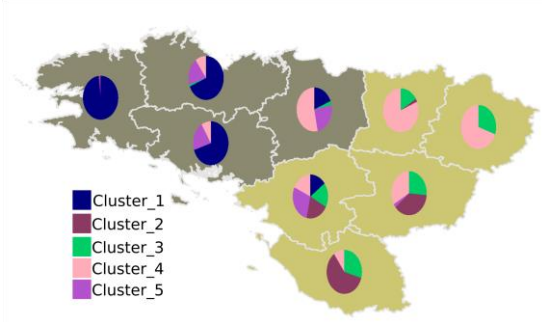
k=6	
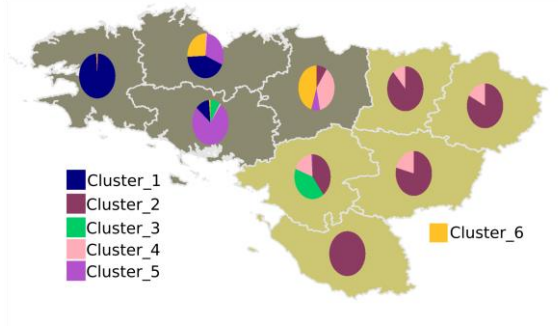	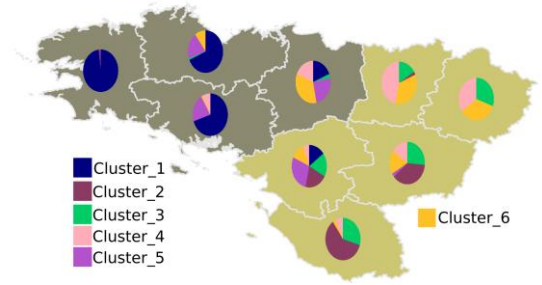
k=7	
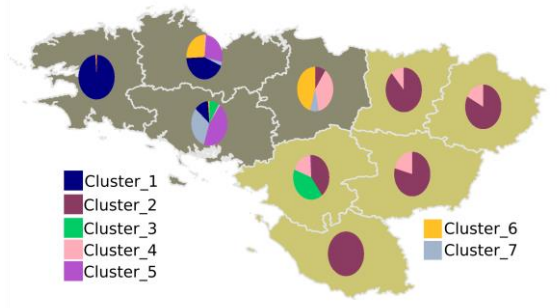	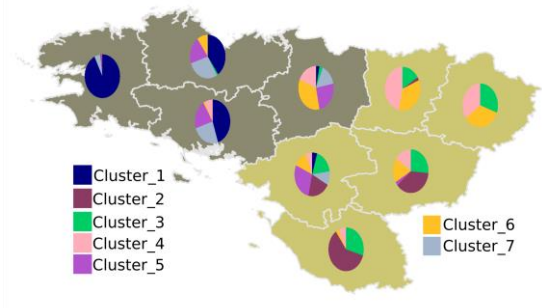
k=8	

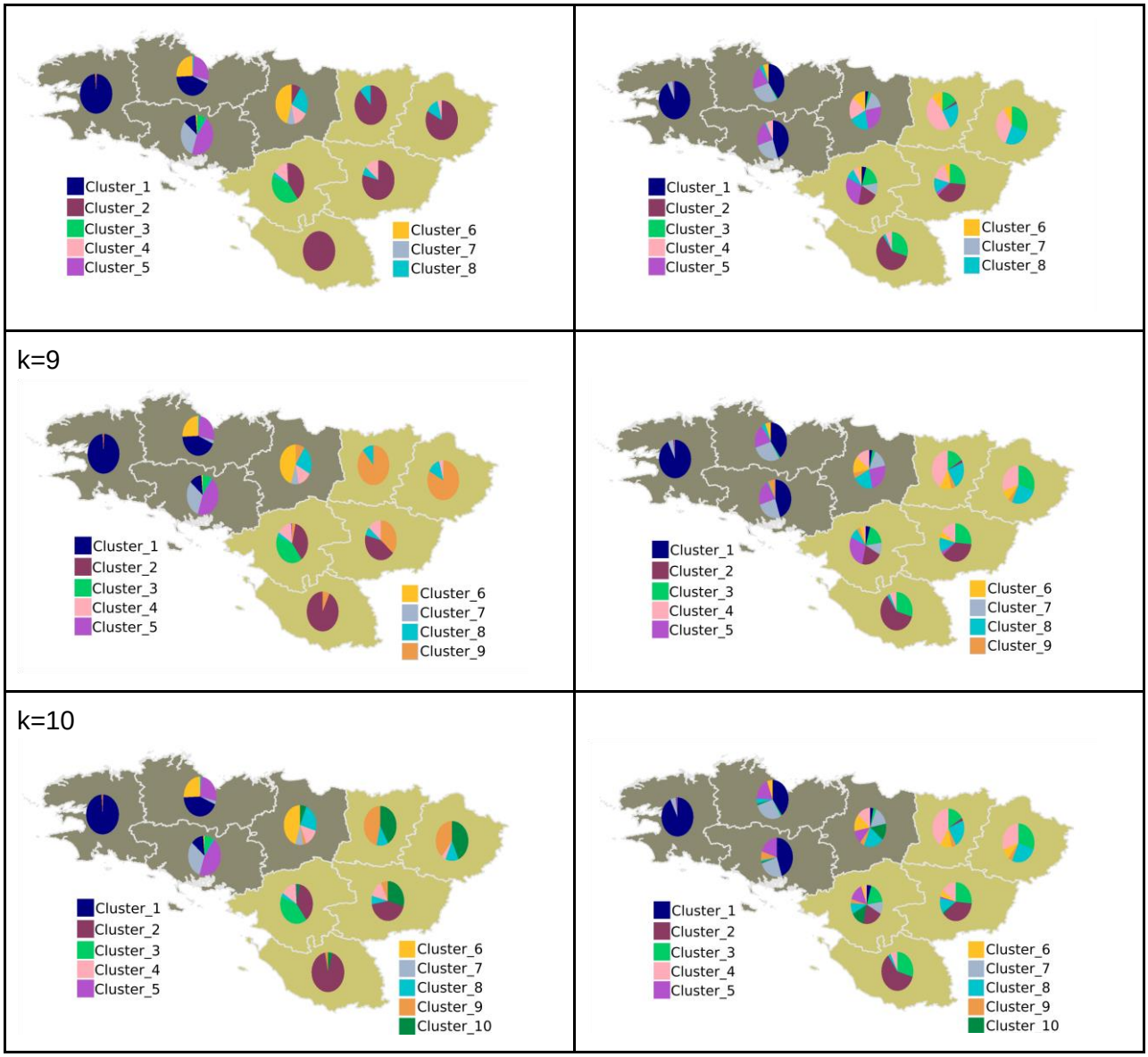

Figure S18**.** Distribution of individuals based on the hierarchical clustering performed on the allele-sharing matrices. Rows show different *k* values used in the hierarchical clustering and columns show the results for different allele count classes. Allele sharing matrices were obtained by randomly selecting 1 million variable sites within each of the two allele count categories and 620 individuals from Northwestern France. Map generated with *R statistical package* using *rgdal, sp, broom, ggplot2 and scatterpie* packages and the "*départements"* boundary dataset from the French platform of open data (https://www.data.gouv.fr/).

MAC 2	MAC 3-10
k=2 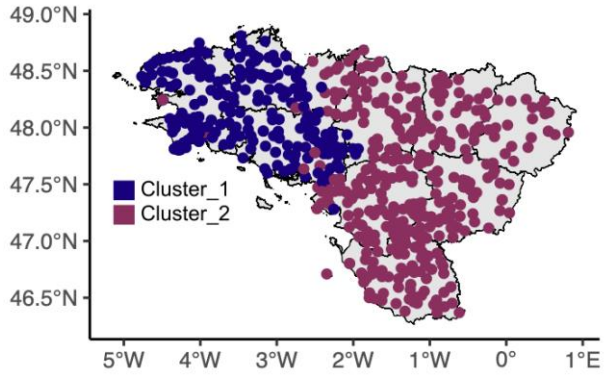	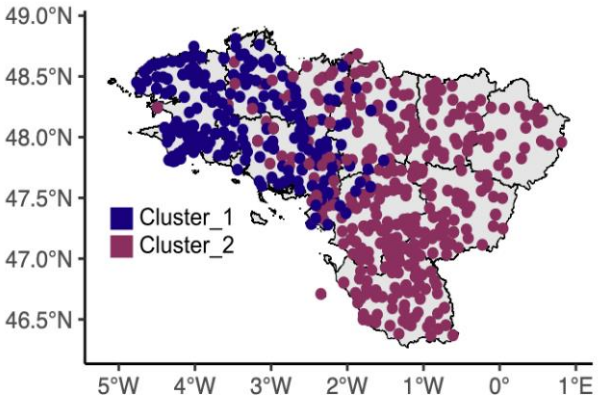
k=3 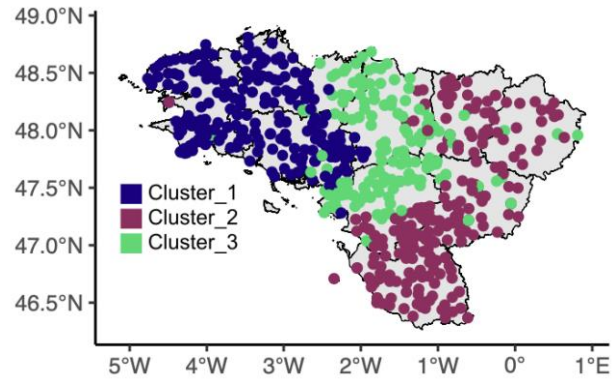	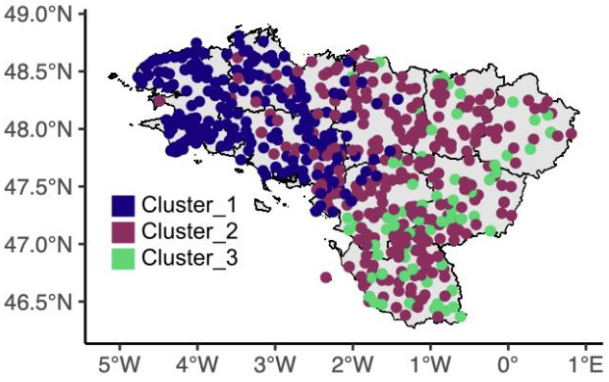
k=4 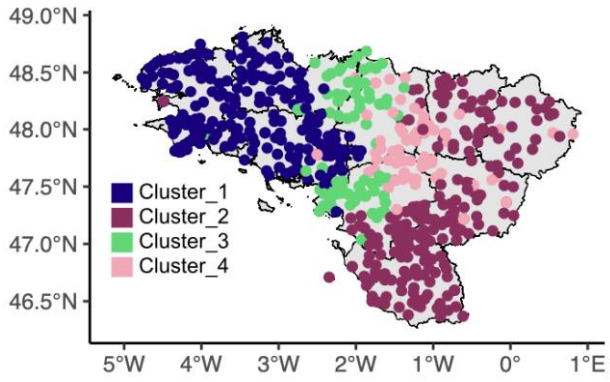	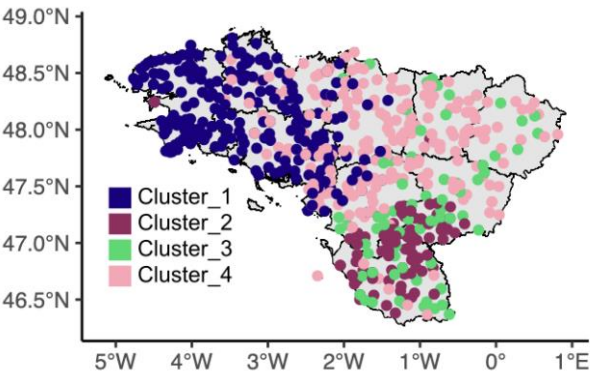
k=5	

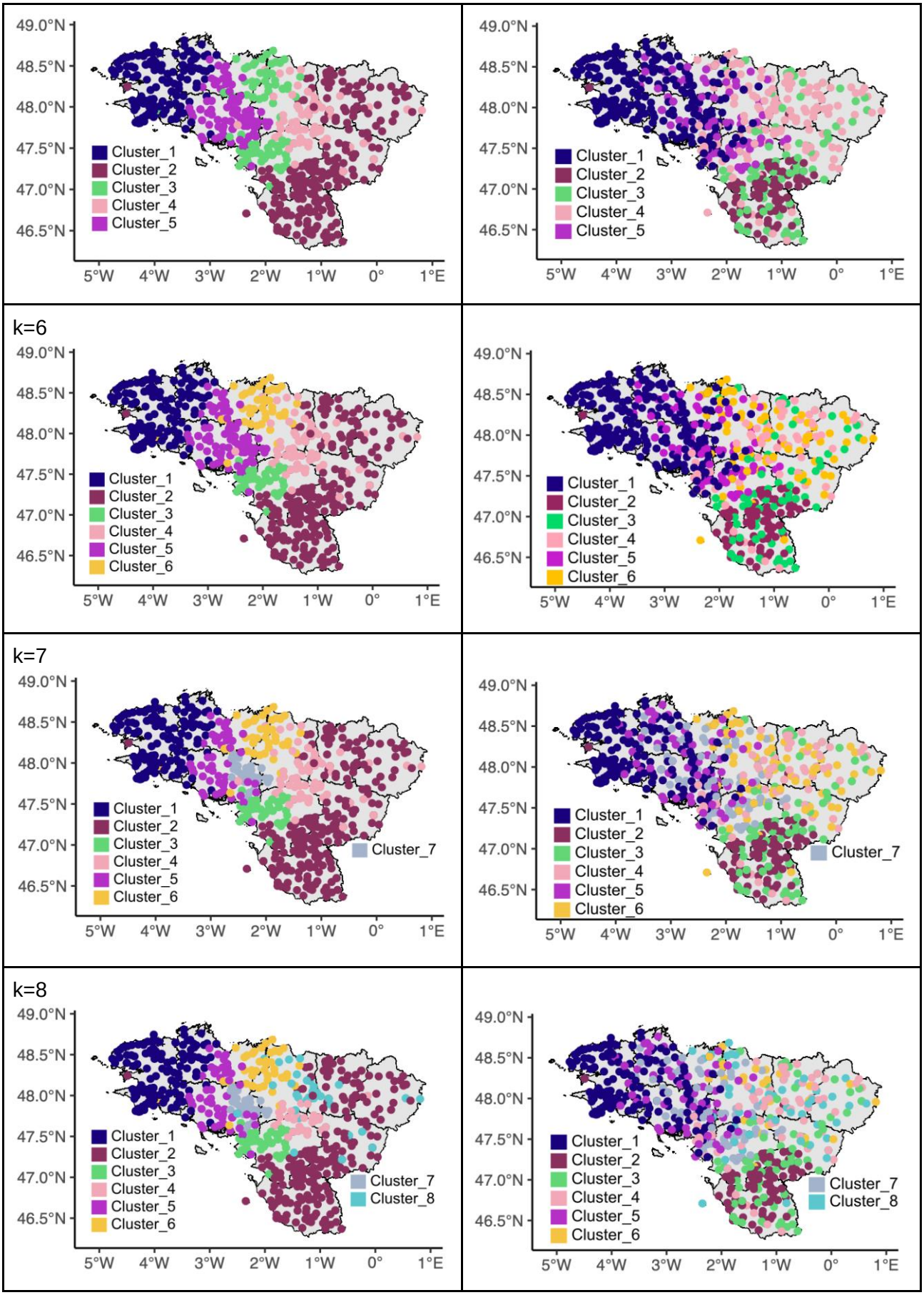
k=6
k=7
k=8
49.0°N
48.5°N
48.0°N
47.5°N
47.0°N
46.5°N
5°W
4°W
3°W
2°W
1°W
0°
1°E
Cluster_1
Cluster_2
Cluster_3
Cluster_4
Cluster_5
Cluster_6
Cluster_7
Cluster_8

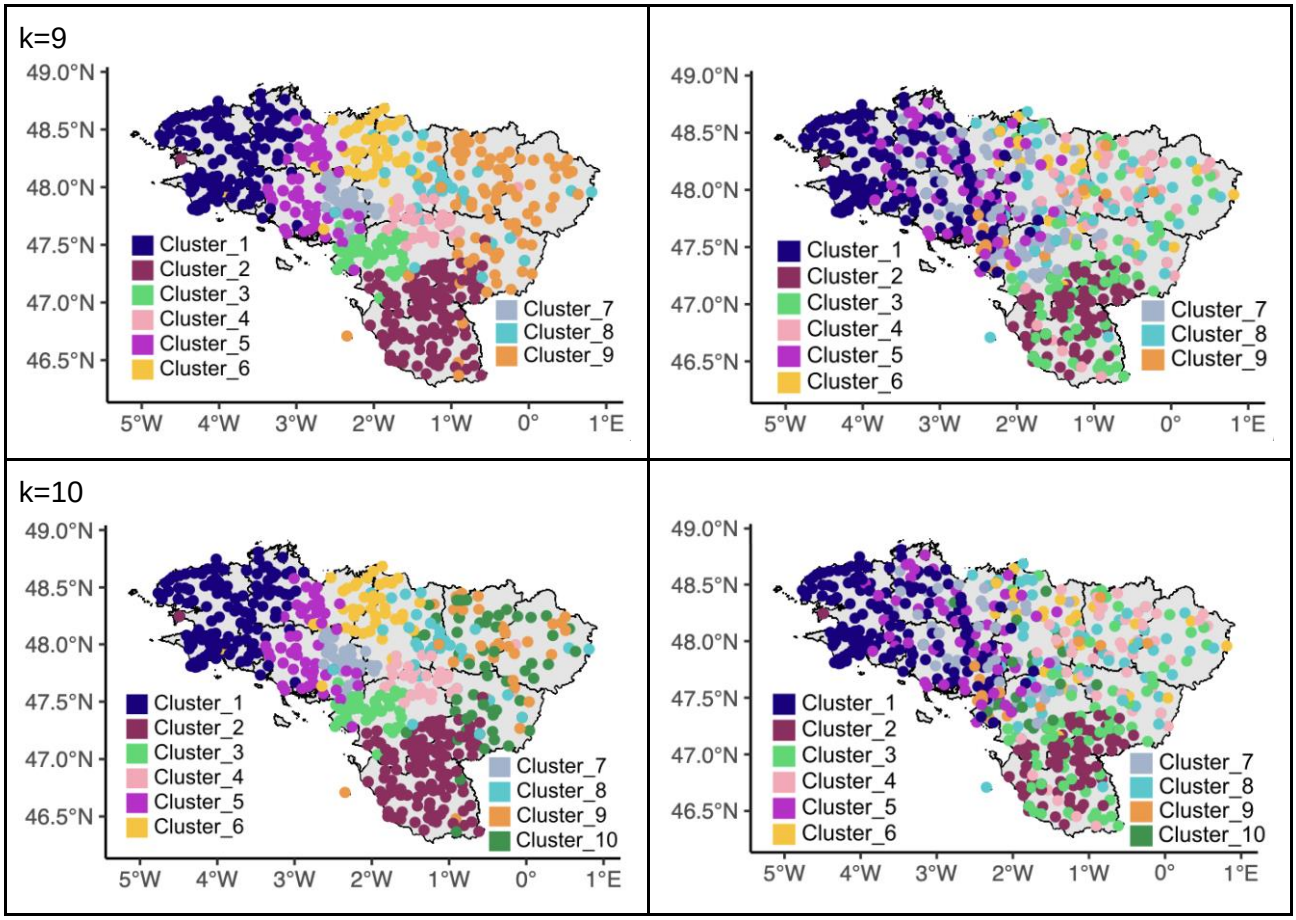

Figure S19. Individual cluster assignment based on the hierarchical clustering performed on the allele-sharing matrices. Rows show different *k* values used in the hierarchical clustering and columns show the results for different allele count classes. Allele sharing matrices were obtained described in Fig. S18 (above). Map generated with *R statistical package* using *rgdal, sp, broom,* and *ggplot2* packages and the "***départements***" boundary dataset from the French platform of open data (https://www.data.gouv.fr/).

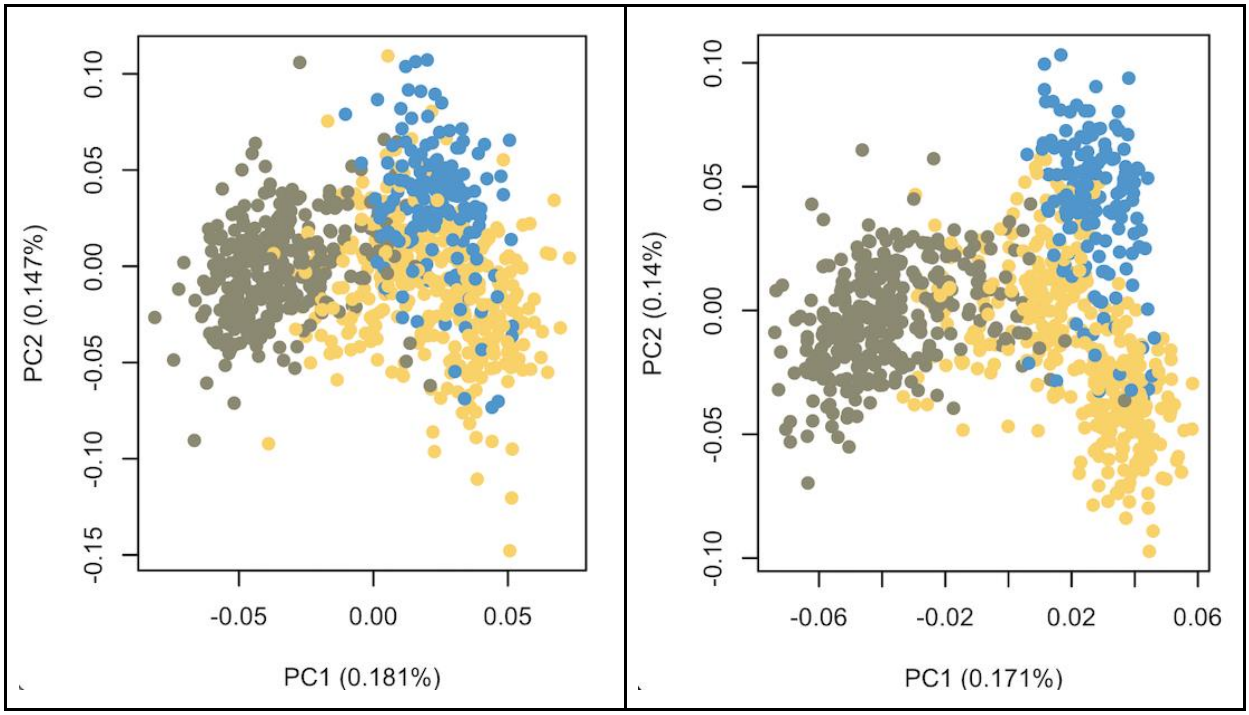

Figure S20. PCA on the WGS dataset containing only French populations for which all the four grandparents belong to the same *commune* (843 samples, Fig. S17). On the left panel, PCA was performed on common sites, MAF > 10% (~443,933 sites). The right panel shows the PCA low-frequency variants (1% < MAF < 10%, ~863,141 sites). Samples from Brittany are coloured in dark green and samples from Northeastern and Southwestern France are coloured in blue and yellow, respectively.

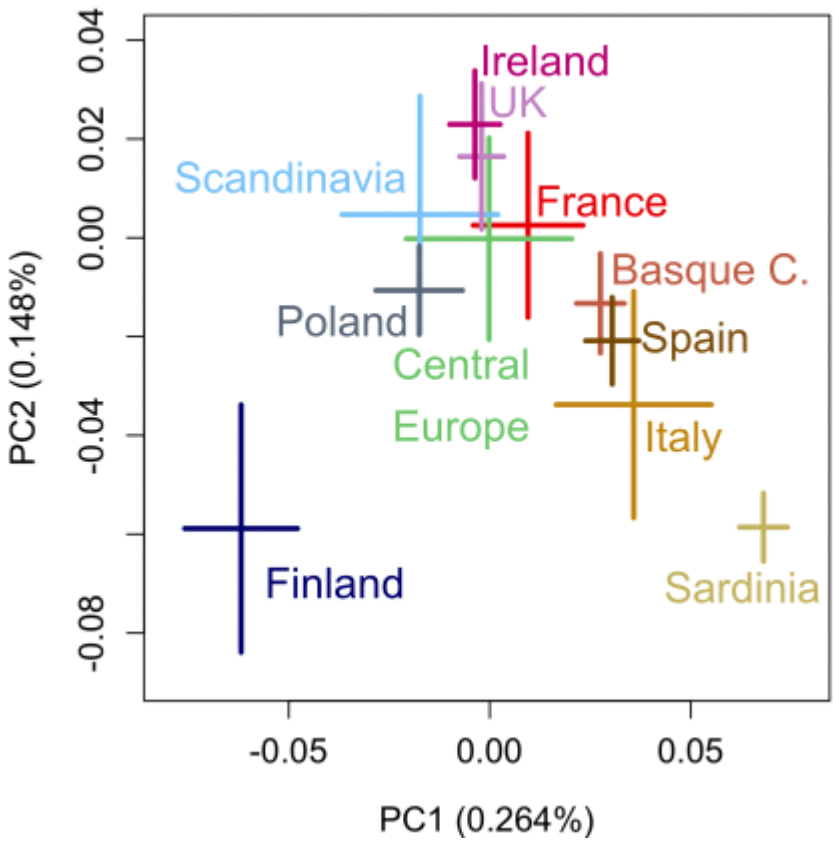

Figure S21. The two first principal components of genetic variation in the “modern merged dataset”, which includes 843 French WGSs (red) for which the birth places of the four grand-parents are situated in close proximity, and genome-wide data from 20 central and western European populations: Basque Country (HGDP), Belgium, Cornwall (UK, POBI), Denmark, Dyfed (UK, POBI), Finland, Germany, Gwynedd (UK, POBI), Ireland, Italy, Kent (UK, POBI), Norfolk (UK, POBI), Northern Ireland, Norway, Orkney Islands (HGDP), Poland, Sardinia (HGDP), Spain, Sweden, United Kingdom. For simpler visualisation samples from Norway, Sweden and Denmark were labelled as “Scandinavia”, samples from Belgium and Germany were labelled as “Central Europe”. All samples from Great Britain are represented by “UK”. Only French samples from the FranceGenRef are shown in the plot. Crosses represent 2*standard deviations of the PC distribution for each group.

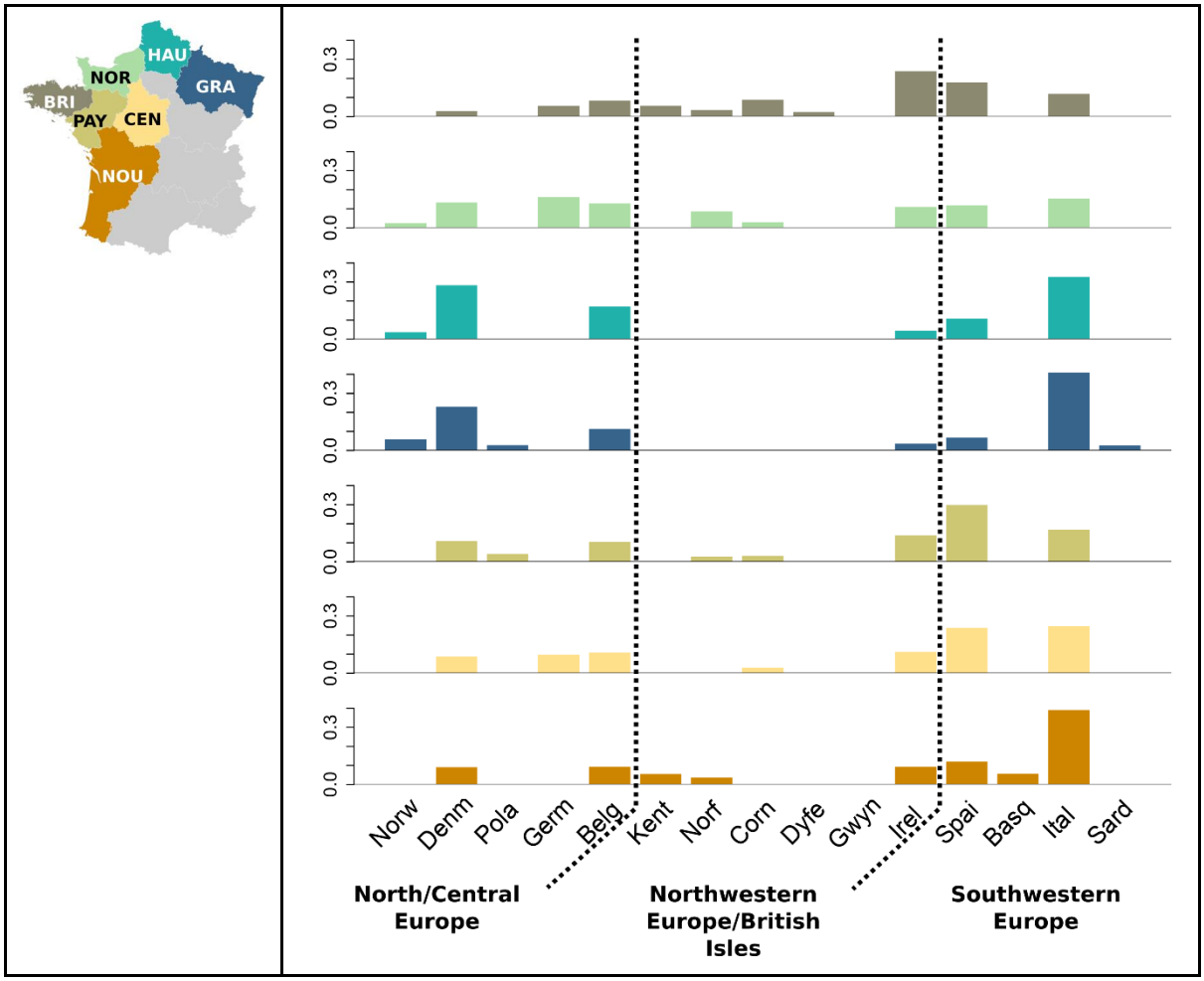

Figure S22. Ancestry profiles obtained with GLOBETROTTER for each of the French regions shown on the left panel (rows). Ancestry contributions shown in the y-axis from each of the European samples in the x-axis. French regions are coloured according to the map on the left pane. Population acronyme: BRI, Brittany; PAY, Pays-de-la-Loire; NOR, Normandy; HAU, Hauts-de-France; GRA, Grand Est; CEN, Centre-Val de Loire; NOU, Nouvelle-Aquitaine. Map generated with *R statistical package* using *sp* packages and the "*régions"* boundary dataset from the French platform of open data (https://www.data.gouv.fr/).

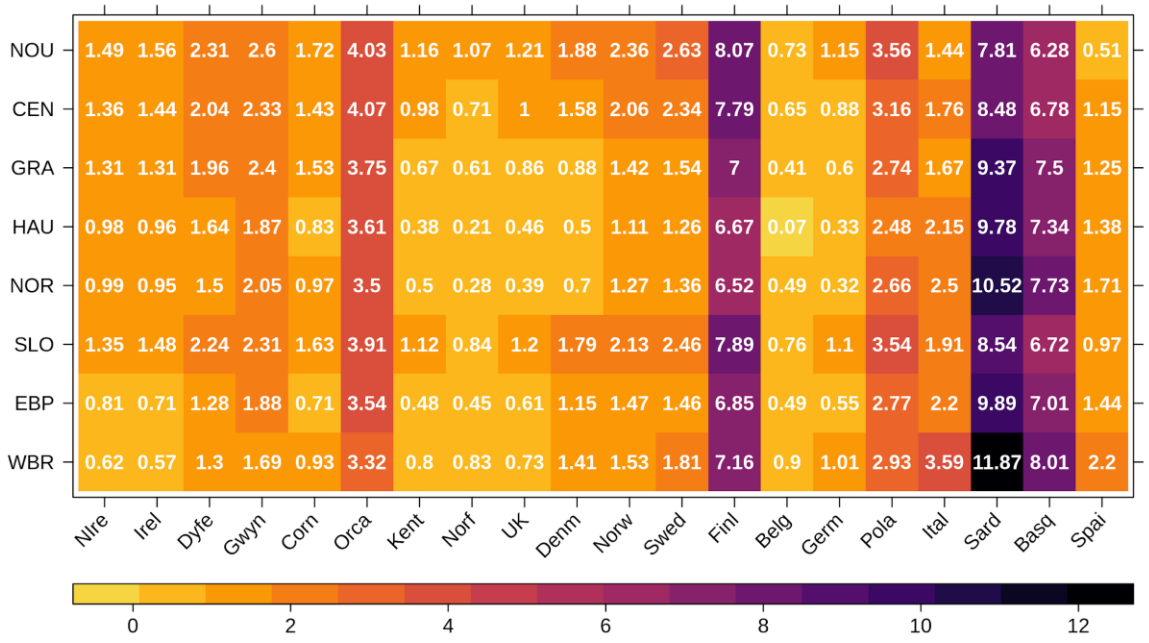

Figure S23. Pairwise average Weir and Cockerham's F_{ST}s between French and other European populations x 1000. French clusters and populations are: WBR, Western Brittany; EBP, Eastern Brittany and Pays-de-la-Loire; SLO, South Loire; NOR, *Normandie*; HAU, Hauts-de-France; GRA, Grand Est; CEN, Centre-Val de Loire; NOU, Nouvelle-Aquitaine. Non-French population acronyms: Basque Country (Basq), Belgium (Belg), Cornwall (Corn), Denmark (Denm), Dyfed (Dyfe), Finland (Finl), Germany (Germ), Gwynedd (Gwyn), Ireland (Irel), Italy (Ital), Kent (Kent), Norfolk (Norf), Northern Ireland (NIrel), Norway (Norw), Orkney Islands (Orca), Poland (Pola), Sardinia (Sard), Spain (Spai), Sweden (Swed), United Kingdom (UK).

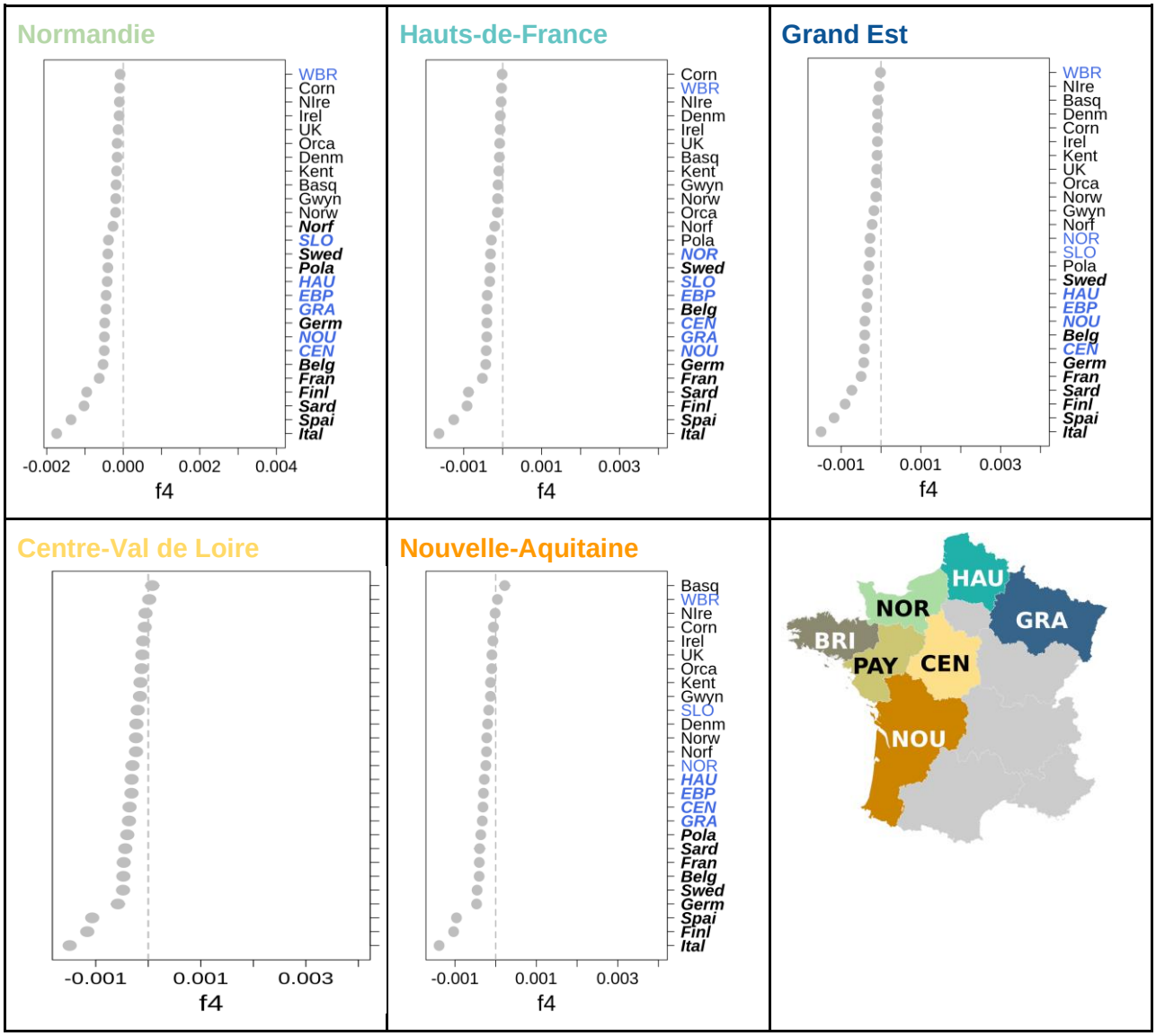

Figure S24**.** *f_4-statistics* of the form *f_4*(Mbuti, French region; Dyfed, X), where the French region is indicated on top of the plot and X is each of the populations on the right side of the plot. *F_4* -statistics values are shown together with one standard deviation. French clusters and populations are: WBR, Western Brittany; EBP, Eastern Brittany and Pays-de-la-Loire; SLO, South Loire; NOR, *Normandie*; HAU, Hauts-de-France; GRA, Grand Est; CEN, Centre-Val de Loire; NOU, Nouvelle-Aquitaine. Ranges correspond to the standard deviation estimated from weighted block jackknife as implemented in *Admixtools*. Map generated with *R statistical package* using *rgdal, sp, broom,* and *ggplot2* packages and the "*départements"* boundary dataset from the French platform of open data (https://www.data.gouv.fr/).

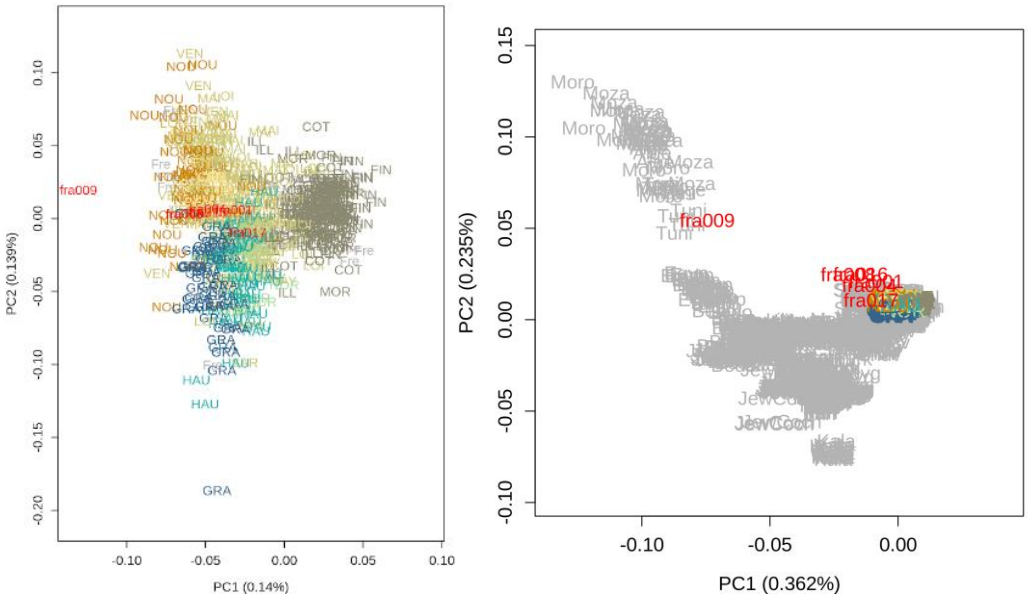

Figure S25. Mediaeval French samples projected onto the two first principal components from present-day Europeans and north Africans. Modern European genotypes present in the Human Origins Array (Reich's Lab, vs.42.2 March 2020 release, (49)) are coloured in grey. Modern French samples analysed in this study are coloured according as in Fig. S24 (above) whereas ancient samples are represented in red. North African sample acronyms: Tuni - Tunisia; Moza - Mozabites; Moro-Morocco. The pca was performed with smartpca (*lsqproject: YES*).

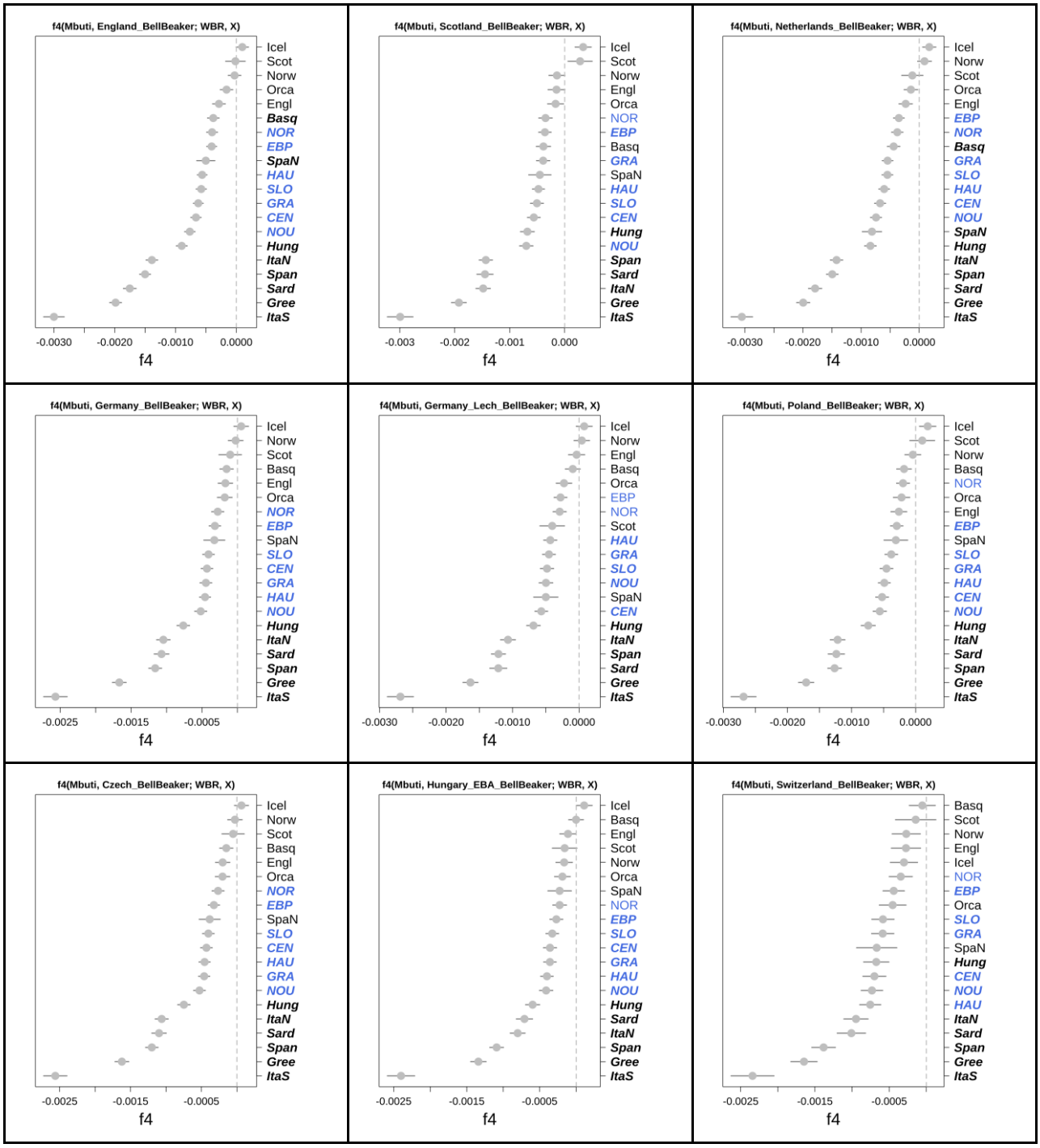
f4(Mbuti, England_BellBeaker; WBR, X)
Icel
Scot
Norw
Orca
Engl
Basq
NOR
EBP
SpaN
HAU
SLO
GRA
CEN
NOU
Hung
ItaN
Span
Sard
Gree
ItaS
-0.0030
-0.0020
-0.0010
0.0000
f4
f4(Mbuti, Scotland_BellBeaker; WBR, X)
Icel
Scot
Norw
Engl
Orca
NOR
EBP
Basq
GRA
SpaN
HAU
SLO
CEN
Hung
NOU
Span
Sard
ItaN
Gree
ItaS
-0.003
-0.002
-0.001
0.000
f4
f4(Mbuti, Netherlands_BellBeaker; WBR, X)
Icel
Norw
Scot
Orca
Engl
EBP
NOR
Basq
GRA
SLO
HAU
CEN
NOU
SpaN
Hung
ItaN
Span
Sard
Gree
ItaS
-0.0030
-0.0020
-0.0010
0.0000
f4
f4(Mbuti, Germany_BellBeaker; WBR, X)
Icel
Norw
Scot
Basq
Engl
Orca
NOR
EBP
SpaN
SLO
CEN
GRA
HAU
NOU
Hung
ItaN
Sard
Span
Gree
ItaS
-0.0025
-0.0015
-0.0005
f4
f4(Mbuti, Germany_Lech_BellBeaker; WBR, X)
Icel
Norw
Engl
Basq
Orca
EBP
NOR
Scot
HAU
GRA
SLO
NOU
SpaN
CEN
Hung
ItaN
Span
Sard
Gree
ItaS
-0.0030
-0.0020
-0.0010
0.0000
f4
f4(Mbuti, Poland_BellBeaker; WBR, X)
Icel
Scot
Norw
Basq
NOR
Orca
Engl
EBP
SpaN
SLO
GRA
HAU
CEN
NOU
Hung
ItaN
Sard
Span
Gree
ItaS
-0.0030
-0.0020
-0.0010
0.0000
f4
f4(Mbuti, Czech_BellBeaker; WBR, X)
Icel
Norw
Scot
Basq
Engl
Orca
NOR
EBP
SpaN
SLO
CEN
HAU
GRA
NOU
Hung
ItaN
Sard
Span
Gree
ItaS
-0.0025
-0.0015
-0.0005
f4
f4(Mbuti, Hungary_EBA_BellBeaker; WBR, X)
Icel
Basq
Engl
Scot
Norw
Orca
SpaN
NOR
EBP
SLO
CEN
GRA
HAU
NOU
Hung
Sard
ItaN
Span
Gree
ItaS
-0.0025
-0.0015
-0.0005
f4
f4(Mbuti, Switzerland_BellBeaker; WBR, X)
Basq
Scot
Norw
Engl
Icel
NOR
EBP
Orca
SLO
GRA
SpaN
Hung
CEN
NOU
HAU
ItaN
Sard
Span
Gree
ItaS
-0.0025
-0.0015
-0.0005
f4

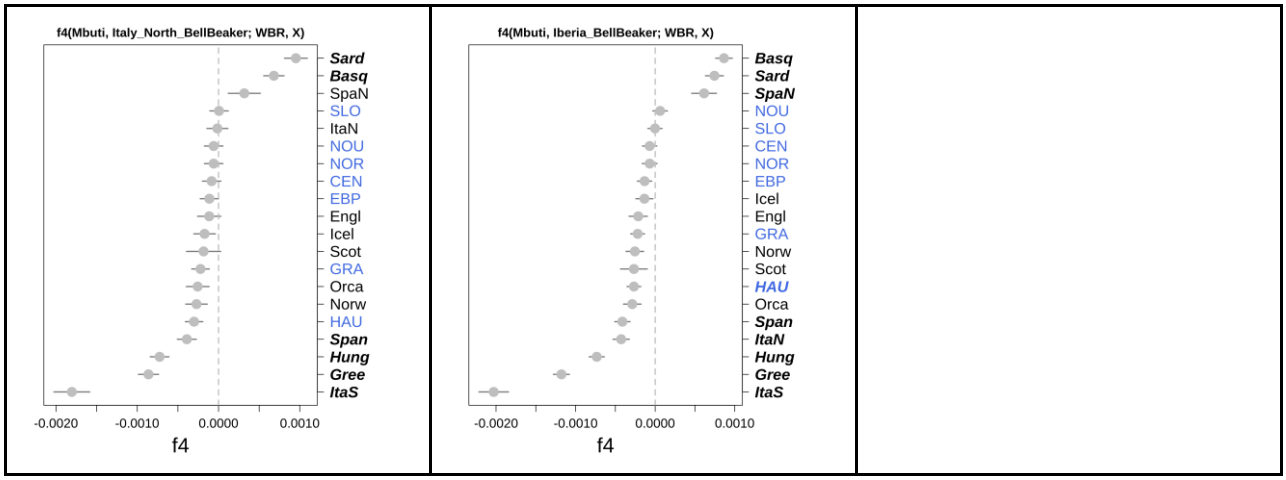

Figure S26. f_4 of the form f_4 *(Mbuti, Bell Beaker population; WBR, X)*, where Bell Beaker population is indicated on top of the plot and X is each of the populations on the y-axis (right side of the plot). French populations are coloured in blue and comparisons with |Z| > 3 are indicated in bold on the y-axis. Ranges correspond to the standard deviation computed from the weighted block jackknife implemented in *Admixtools*.

Supplementary Tables

Table S1. Summary of the admixture composition, sources and times for the French regions obtained with GLOBETROTTER

				Admixture event 1			Admixture event 2		
French region	Best Fitting Admixture Model	Goodness of fit (R^2)	Time* of admixture in ya [95% CI]	Minor Component	Major Component	Ratio	Minor Component	Major Component	Ratio
Brittany (BRI)	One-date-multiway	0.62	1047 [858-1244]	Italy	Kent	0.32:0.68	Kent	Kent	0.43:0.57
Pays-de-la-Loire (PAY)	One-date-multiway	0.70	1337 [1163-1554]	Italy	Kent	0.49:0.51	Kent	Spain	0.48:0.52
Centre et Val-Loire (CEN)	Unclear signal	0.19	NA	NA	NA	NA	NA	NA	NA
Normandy (NOR)	One-date-multiway	0.30	1035 [733-1293]	Denmark (Denm)	Italy (Ital)	0.47:0.53	Ireland (Irel)	Norfolk (Norf)	0.24:0.76
Hauts-de-France (HAU)	One-date	0.65	1105[951-1354]	Italy	Kent	0.49:0.51	NA	NA	NA
Grand Est (GRA)	One-date	0.50	1148 [925-1438]	Kent (Kent)	Italy (Ital)	0.47:0.53	NA	NA	NA
Nouvelle-Aquitaine (NOU)	One-date-multiway	0.35	1540 [887-1914]	Kent	Spain	0.31:0.69	Kent	Italy	0.42:0.58

*Times were converted from generations to years ago using a generation time of 29 years/generation.

Table S2. Summary of the ancient DNA Mediaeval samples from France sequenced in this study

Samples ID	Dates*	Place	% endog.	Mapped reads	3' and 5' damage %	Average read length	Genome cov.**	Gender***	X-contam. (SE)	mtDNA contam.	total sites HOA	mean cov.
fra001	375-541 cal. AD	Saint Lupien Rezé	0.199312	271,093,228	16.9-17.3	75.38	0.48	XX	NA	0.01	247020	0.551608
fra004	414-553 cal. AD	Saint Lupien Rezé	0.057764	15,241,917	14.2-15.0	72.26	0.28	XY	0.04367 (0.009)	0.02	169051	0.344645
fra008	943 - 1024 cal. AD	Chaussé Saint Pierre - Angers	0.018284	5,983,204	25.1-25.6	55.97	0.08	consistent with XY but not XX	0.22336 (0.000)	0.01	64438	0.116075
fra009	414-548 cal. AD	Chaussé Saint Pierre - Angers	0.276266	26,781,466	23.6-23.8	70.51	0.36	XY	0.03787 (0.007)	0.01	199735	0.421043
fra016	600-700 AD	Chémeré	0.480058	234,557,159	24.3-24.5	56.46	3.43	consistent with XY but not XX	0.014 (0.001)	0.01	574582	4.153501
fra017	600-700 AD	Chémeré	0.020224	6,559,927	9.1-11.1	80.88	0.14	XY	0.10887 (0.000)	0.01	92736	0.170474

* cal. AD = Radiocarbon calibrated Anno Domini (AD); Anno Domini based on the archaeological context

** after MapQ 30 filtering

*** estimated biological sex from alignment data (1).

%endog. - % of endogenous DNA.

Table S3. qpAdm p-values (X^2) for one-way models for modern and Mediaeval French

	WBR (n=25)	**EBP** (n=25)	**SLO** (n=25)	**NOR** (n=19)	**HAU** (n=25)	**GRA** (n=25)	**CEN** (n=25)	**NOU** (n=25)	Mediaeval French (fra001, fra004, fra008, fra016, fra017)
England_Roman	**0.9362**	**0.4472**	0.0008	**0.4504**	**0.3048**	0.0004	0.0017	0.0000	**0.1011**
England_Saxon	0.0002	0.0000	0.0000	0.0000	0.0000	0.0000	0.0000	0.0000	0.0002
Germany_EMedieval	**0.0744**	**0.1378**	0.0000	**0.0872**	0.0054	0.0000	0.0000	0.0000	**0.0756**
Iberia_Celtiberian	0.0001	0.0000	0.0008	0.0002	0.0004	0.0000	0.0004	0.0028	0.0470
Iberia_Medieval_published	0.0000	0.0004	0.0366	0.0004	0.0009	0.0277	0.0219	**0.0696**	**0.2434**
Iberia_Carolingian	**0.2219**	**0.4450**	**0.5731**	**0.5007**	**0.5409**	**0.4385**	**0.5462**	**0.6125**	**0.9324**
Iberia_Visigoth_Barcelona	**0.0689**	**0.1855**	**0.3636**	**0.1046**	**0.3221**	**0.3306**	**0.3678**	**0.4429**	**0.7020**
Iberia_Visigoth_Girona	0.0363	**0.2358**	**0.9075**	**0.3527**	**0.3833**	**0.7244**	**0.5947**	**0.7063**	**0.9538**
Iceland_Early_Christian	**0.3617**	**0.2317**	0.0280	**0.1455**	**0.1442**	0.0442	0.0219	0.0009	**0.2354**
Iceland_Pre_Christian	0.0000	0.0000	0.0000	0.0000	0.0000	0.0000	0.0000	0.0000	0.0000
Italy_Medieval_EarlyModern_oCentralEuropean	0.0000	0.0002	**0.4682**	0.0003	0.0002	**0.6033**	**0.3087**	**0.0695**	**0.8164**
Italy_Medieval_EarlyModern	0.0000	0.0000	0.0000	0.0000	0.0000	0.0000	0.0000	0.0000	0.0000
Italy_North_EarlyMedieval_Langobards	0.0000	0.0000	0.0000	0.0000	0.0000	0.0000	0.0000	0.0000	**0.4315**
Vikings	0.0039	0.0000	0.0000	0.0000	0.0000	0.0000	0.0000	0.0000	0.0027

Present-day population/cluster acronyms: Western Brittany (WBR), Eastern Brittany/*Pays-de-la-Loire* (EBP), south Loire (SLO), Normandy *(*NOR*)*; *Hauts-de-France* (HAU); *Grand Est (*GRA*)*; *Centre-Val de Loire (*CEN*)*; *Nouvelle-Aquitaine (*NOU*).* Ancient sample sizes are shown in Fig. 4. Non-significant p-values are shown in bold.

Table S4. *qpAdm* results for the three-way model assuming Steppe pastoralists (SP), Early Farmers (EF) and Western Hunter-Gatherers (WHG) as sources populations of each modern and Mediaeval French populations (FRMedieval)

	SP (n=17)	EF (n=73)	WHG (n=42)			
	Prop (std. error)	Prop (std. error)	Prop (std. error)	d.f	X^2	p-value(X^2)
WBR (n=25)	0.460 (0.021)	0.436 (0.020)	0.104 (0.010)	10	77.265	1.72E-12
EBP (n=25)	0.435 (0.021)	0.476 (0.020)	0.089 (0.009)	10	69.372	5.86E-11
SLO (n=25)	0.372 (0.021)	0.545 (0.020)	0.083 (0.010)	10	63.73	7.09E-10
NOR (n=19)	0.437 (0.021)	0.480 (0.020)	0.083 (0.010)	10	51.303	1.54E-07
HAU (n=25)	0.422 (0.021)	0.483 (0.020)	0.095 (0.010)	10	67.78	1.19E-10
GRA (n=25)	0.389 (0.020)	0.548 (0.019)	0.063 (0.009)	10	64.295	5.53E-10
CEN (n=25)	0.384 (0.020)	0.538 (0.020)	0.079 (0.010)	10	70.677	3.28E-11
NOU (n=25)	0.329 (0.019)	0.578 (0.019)	0.093 (0.009)	10	59.818	3.92E-09
Mediaeval French (n=5)	0.326 (0.057)	0.608 (0.054)	0.067 (0.029)	10	9.248	0.508768613

Table S5 - *f_4-statistics* of the form *f_4(Mbuti; ancient EUR sample; WBR, other modern French population)*

Pop1 (W)	Pop2 (X) :	Pop3 (Y)	Pop4 (Z)	D-stat	Z	BABA	ABBA	# of SNPs
Mbuti	**Russia_EBA_Yamnaya_Samara**	**WBR**	**NOU**	**-0.0091**	**-11.381**	**27968**	**28481**	**464380**
Mbuti	**Russia_EBA_Yamnaya_Samara**	**WBR**	**CEN**	**-0.007**	**-8.586**	**28029**	**28422**	**464380**
Mbuti	**Russia_EBA_Yamnaya_Samara**	**WBR**	**SLO**	**-0.0069**	**-8.816**	**28020**	**28407**	**464380**
Mbuti	**Russia_EBA_Yamnaya_Samara**	**WBR**	**GRA**	**-0.0058**	**-7.646**	**28068**	**28398**	**464380**
Mbuti	**Russia_EBA_Yamnaya_Samara**	**WBR**	**HAU**	**-0.0053**	**-7.279**	**28085**	**28383**	**464380**
Mbuti	**Russia_EBA_Yamnaya_Samara**	**WBR**	**NOR**	**-0.0041**	**-4.895**	**28093**	**28326**	**464380**
Mbuti	**Russia_EBA_Yamnaya_Samara**	**WBR**	**EBR**	**-0.0041**	**-5.3**	**28108**	**28341**	**464380**
Mbuti	Germany_EN_LBK_published	WBR	HAU	-0.0004	-0.47	28132	28152	463062
Mbuti	Germany_EN_LBK_published	WBR	NOR	-0.0003	-0.429	28103	28122	463062
Mbuti	Germany_EN_LBK_published	WBR	EBR	0.0003	0.37	28139	28123	463062
Mbuti	Germany_EN_LBK_published	WBR	GRA	0.0013	1.678	28189	28115	463062
Mbuti	Germany_EN_LBK_published	WBR	CEN	0.0021	2.66	28213	28096	463062
Mbuti	**Germany_EN_LBK_published**	**WBR**	**NOU**	**0.0025**	**3.267**	**28231**	**28089**	**463062**
Mbuti	**Germany_EN_LBK_published**	**WBR**	**SLO**	**0.0026**	**3.384**	**28218**	**28070**	**463062**
Mbuti	Iberia_EN	WBR	HAU	-0.0009	-1.089	27436	27484	452926
Mbuti	Iberia_EN	WBR	EBR	-0.0001	-0.179	27443	27451	452926
Mbuti	Iberia_EN	WBR	NOR	0.0006	0.721	27451	27417	452926
Mbuti	Iberia_EN	WBR	GRA	0.0013	1.654	27508	27434	452926
Mbuti	Iberia_EN	WBR	CEN	0.0015	1.831	27512	27428	452926
Mbuti	Iberia_EN	WBR	SLO	0.0021	2.638	27515	27402	452926
Mbuti	**Iberia_EN**	**WBR**	**NOU**	**0.0032**	**3.944**	**27569**	**27392**	**452926**
Mbuti	**Luxembourg_Loschbour_published.DG**	**WBR**	**GRA**	**-0.0064**	**-5.314**	**28402**	**28769**	**466881**
Mbuti	**Luxembourg_Loschbour_published.DG**	**WBR**	**NOU**	**-0.0041**	**-3.444**	**28477**	**28713**	**466881**
Mbuti	Luxembourg_Loschbour_published.DG	WBR	CEN	-0.0034	-2.883	28494	28689	466881
Mbuti	Luxembourg_Loschbour_published.DG	WBR	HAU	-0.003	-2.565	28504	28677	466881
Mbuti	Luxembourg_Loschbour_published.DG	WBR	SLO	-0.0026	-2.17	28513	28661	466881
Mbuti	Luxembourg_Loschbour_published.DG	WBR	NOR	-0.0021	-1.702	28508	28627	466881
Mbuti	Luxembourg_Loschbour_published.DG	WBR	EBR	-0.0019	-1.557	28533	28641	466881

Note: significant values (|Z| > 3) are indicated in bold; |Z| > 4 are indicated in yellow and |Z| > 6 are indicated in red.

Table S6 - *F_4-statistics* of the form *f_4(Mbuti; Megalithic samples; WBR, other modern French populations)*

Pop1 (W)	Pop2 (X) :	Pop3 (Y)	Pop4 (Z)	D-stat	Z	BABA	ABBA	# of SNPs
Mbuti	Ireland_Megalithic.SG	WBR	English	-0.000207	-1.648	28628	28726	471404
Mbuti	Ireland_Megalithic.SG	WBR	HAU	-0.000153	-1.59	28687	28759	471404
Mbuti	Ireland_Megalithic.SG	WBR	GRA	-0.000106	-1.092	28705	28755	471404
Mbuti	Ireland_Megalithic.SG	WBR	NOR	-0.000054	-0.527	28681	28707	471404
Mbuti	Ireland_Megalithic.SG	WBR	EBP	-0.000031	-0.325	28707	28722	471404
Mbuti	Ireland_Megalithic.SG	WBR	SLO	0.00009	0.916	28745	28703	471404
Mbuti	Ireland_Megalithic.SG	WBR	CEN	0.000095	0.96	28759	28714	471404
Mbuti	Ireland_Megalithic.SG	WBR	NOU	0.000196	2.023	28788	28696	471404
Mbuti	Scotland_Megalithic.SG	WBR	HAU	-0.000144	-1.007	9333	9355	154275
Mbuti	Scotland_Megalithic.SG	WBR	GRA	-0.000104	-0.72	9340	9356	154275
Mbuti	Scotland_Megalithic.SG	WBR	English	-0.000133	-0.684	9317	9338	154275
Mbuti	Scotland_Megalithic.SG	WBR	NOR	-0.000088	-0.577	9328	9342	154275
Mbuti	Scotland_Megalithic.SG	WBR	EBP	-0.000079	-0.555	9332	9344	154275
Mbuti	Scotland_Megalithic.SG	WBR	CEN	-0.000014	-0.091	9350	9352	154275
Mbuti	Scotland_Megalithic.SG	WBR	SLO	0.000103	0.695	9350	9334	154275
Mbuti	Scotland_Megalithic.SG	WBR	NOU	0.000316	2.098	9376	9327	154275

Note: Significant differences in allele sharing would result in |Z| > 3, which was not found for any of the above comparisons.

Table S7 - F_4-statistics of the form *f_4(Mbuti; ancient EUR sample; WBR, other modern French population)*								
Pop1 (W)	Pop2 (X) :	Pop3 (Y)	Pop4 (Z)	D-stat	Z	BABA	ABBA	# of SNPs
Mbuti	**Germany_CordedWare**	**WBR**	**GRA**	**-0.00640**	**-8.235**	**28300**	**28666**	**466547**
Mbuti	**Germany_CordedWare**	**WBR**	**NOR**	**-0.00480**	**-5.766**	**28320**	**28592**	**466547**
Mbuti	**Germany_CordedWare**	**WBR**	**CEN**	**-0.00730**	**-9.113**	**28269**	**28687**	**466547**
Mbuti	**Germany_CordedWare**	**WBR**	**EBR**	**-0.00460**	**-5.987**	**28343**	**28604**	**466547**
Mbuti	**Germany_CordedWare**	**WBR**	**SLO**	**-0.00650**	**-8.191**	**28285**	**28653**	**466547**
Mbuti	**Germany_CordedWare**	**WBR**	**NOU**	**-0.00880**	**-10.708**	**28224**	**28724**	**466547**
Mbuti	**Germany_CordedWare**	**WBR**	**HAU**	**-0.00620**	**-8.223**	**28302**	**28658**	**466547**

Table S8- f_4-statistics of the form *f_4(Mbuti; modern French population; Iberian Early Neolithic, Early Neolithic LBK)*

Pop1 (W)	Pop2 (X) :	Pop3 (Y)	Pop4 (Z)	D-stat	Z	BABA	ABBA	# of SNPs
Mbuti	EBP	Iberia_EN	Germany_EN_LBK_published	-0.000084	-0.43	26520	26558	447696
Mbuti	WBR	Iberia_EN	Germany_EN_LBK_published	-0.000141	-0.716	26504	26567	447696
Mbuti	NOR	Iberia_EN	Germany_EN_LBK_published	-0.000251	-1.257	26470	26583	447696
Mbuti	HAU	Iberia_EN	Germany_EN_LBK_published	-0.000063	-0.317	26501	26529	447696
Mbuti	GRA	Iberia_EN	Germany_EN_LBK_published	-0.000136	-0.692	26512	26572	447696
Mbuti	SLO	Iberia_EN	Germany_EN_LBK_published	-0.000056	-0.279	26529	26553	447696
Mbuti	CEN	Iberia_EN	Germany_EN_LBK_published	-0.000076	-0.388	26523	26557	447696
Mbuti	NOU	Iberia_EN	Germany_EN_LBK_published	-0.000214	-1.098	26493	26589	447696

Note: Significant differences in allele sharing would result in |Z| > 3, which was not found for any of the above comparisons.

Supplementary Notes

Supplementary archaeological details

Rezé (Loire-Atlantique) - Saint-Lupien area

Rezé is located in the *département* of *Loire Atlantique* on the southern shore of the Loire river facing the city of Nantes to the north. It is located at ~55km from the Atlantic coast. The excavation was carried out by the team of Mikaël Rouzic between 2005 and 2016 and the archaeological description of the sites remains unpublished.

Site: MR 4825
Samples: SP 4903 (fra001)
Radiocarbon dating: 375-541 cal AD

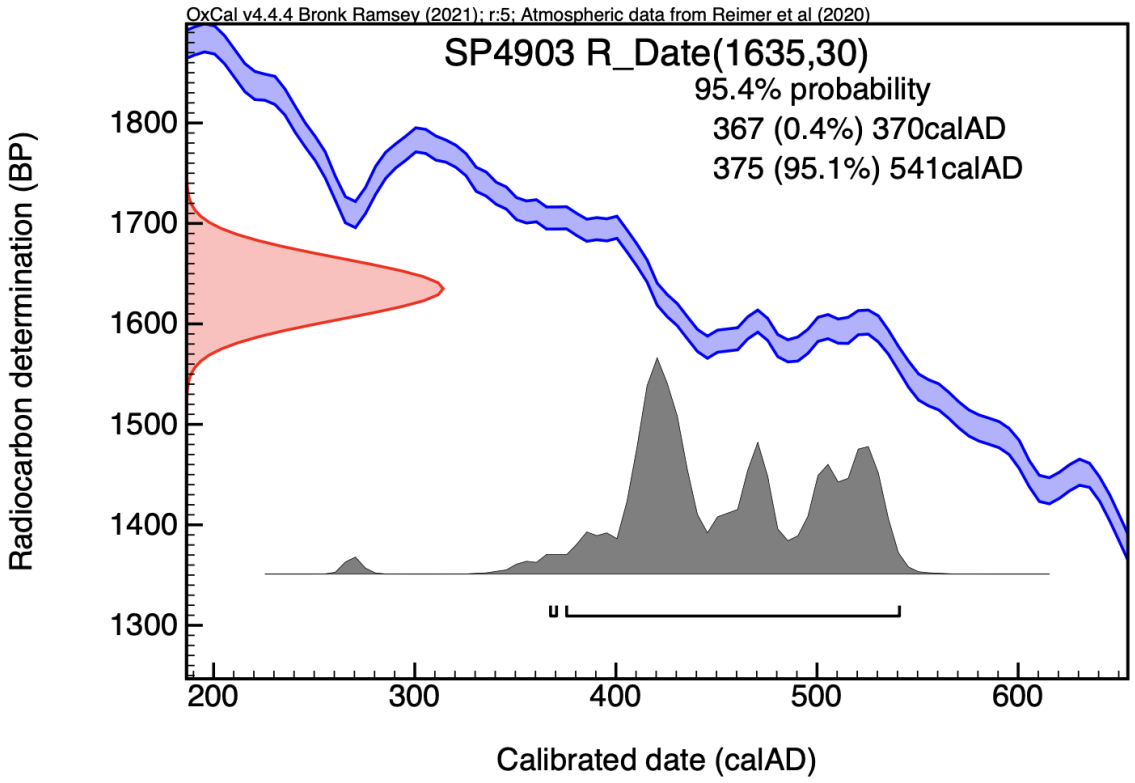

Figure S27: age graph of individual fra001 radiocarbon dating.

The wall of the site MR 4825 was pitted on several layers in order to install the SP 4903 grave with no signs of excavation. The grave was filled with a compact and heterogeneous brown silt, very rich in TCA, lime, gravel and coal. The grave contained the individual SP4903 and two ceramic shards were found inside. The individual was an adult who died at an age of 20-59 years.

Site: US 20380; US 20381; US 20382; US 20383
Samples: SP 20380 (fra004)
Radiocarbon Dating: 414-553 cal AD

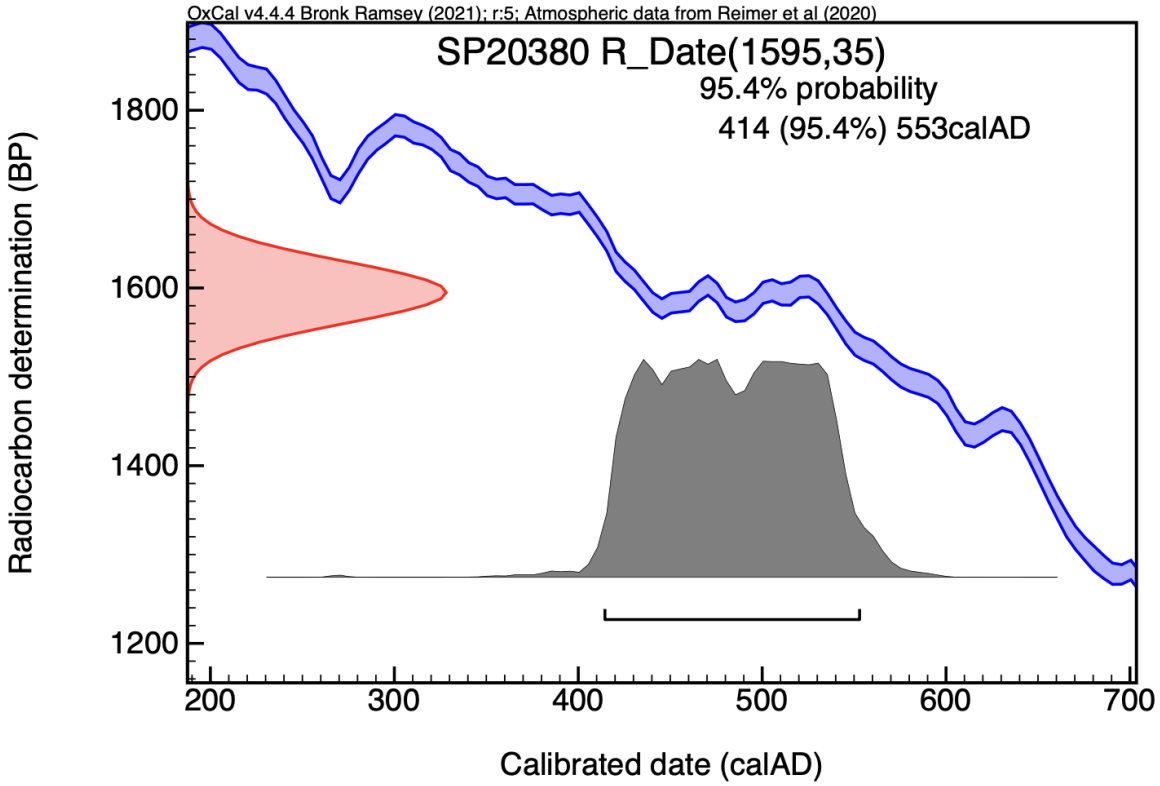

Figure S28: age graph of individual fra004 radiocarbon dating

The site consists of a 2.40 m long and 0.72 m wide burial pit, oriented east/west. It was dug in the ancient road and lies on top of an ash and charcoal layer. The fill is a compact and heterogeneous medium brown sandy loam containing numerous inclusions of architectural terracotta fragments, small blocks, some mortar fragments, several shards of ancient ceramics, glass and faunal bones. Six nails and eight shanks of carpentry nails were taken from the entire thickness of the filling. The skeleton remnants found inside belonged to a male individual 20-29 years old at death.

Chéméré *(Loire-Atlantique)*

Samples: SP 46 and SP 55 (fra016 and fra017)
Dates based on the archaeological context: 600-700 AD

The Merovingian necropolis of Chéméré (*Loire Atlantique*, south Nantes) is located in an area peripheral to the present village. Its occupation is dated to the 6th-7th centuries by the furniture deposited in the tombs and by radiocarbon-based analyses. The total surface area of the burial space is estimated to be around 7700 m². Approximately 1500 m² of land containing 416 tombs have been cleared since the 1960s. The latest excavations in 2007 yielded a population sample of 181 individuals (155 adults and 26 children) recognised by anthropological analysis as a morphologically homogenous group. The two men 46 and 55 are from this group. They were buried in the same row, at the southern end of the cemetery.

Angers (Maine-et-Loire) - Chaussé Saint Pierre
Samples: SP 1046 and SP 1049A (fra008 and fra009)
Radiocarbon calibrated (cal.) dates: 943 - 1024 cal. AD and 414-548 cal. CE

The site of Chaussé Saint-Pierre is located right in the modern city-center of Angers. The city of Angers is located on the intersection of Maine and the Loire rivers and on the northern shore of the latter. It is situated approximately 100km upstream from Nantes. The excavations in this site, which were led by the team of Martin Pithon, from the INRAP of west France, took place between July and August 2009.
The large density of archaeological remains around the Chaussé Saint-Pierre suggests it was densely occupied from the first period of the Roman Empire (27 BCE-250 CE). Until the 4th century CE the area was occupied by commercial buildings and thermes, nevertheless by the 5th century archaeological remains associated with a necropolis indicate a shift in the pattern of occupation. The excavation of Rue Chaussée-Saint-Pierre focused on the north-eastern end of the hopper where the project was the deepest and where the remains were best preserved. The excavations investigated a stratigraphic sequence of almost 1 m thick between the modern-day earthworks and the natural terrain over an area of ~100 m^2. The analysis of this sequence shows five main phases of occupation which lie within a chronological interval between the beginning of the Roman Empire (20 BC to 15 AD) and the modern period. Funerary-associated occupation begins in phase three.

SP 1049A (fra009)

The burial SP 1049 is among the earliest among those belonging to the phase three of occupation and the dating ranges from the beginning of the 5th century to the first half of the 6th century. This tomb, which has been badly damaged by Medieval/modern construction, seems to be part of a homogeneous group of six burials very similar in nature. The dating of the tomb shows repeated burial and skeletal remains indicate the presence of a total of three individuals, two adults and one child. The child's skeleton and one skull not belonging to the child have been dated to 401-539 cal AD and 414-548 cal. AD, respectively (https://dolia.inrap.fr/flora/ark:/64298/0121736 in French). The skeleton remains indicate the child was buried at the age of 1-4 years old. The other skeletal remains seem to belong to a female and an individual of indeterminate gender aged of >25 and >30 years, respectively. The time proximity of the burials within the tomb are likely indicative of a voluntary grouping and may represent a family management of the deposits.

SP 1046 (fra008)

The tomb SP 1046 together with a set of the other tombs dating from the 13-15th century CE indicate the practice of reuse of the tombs. The burial site is composed of heterogeneous loose deposits of fine sandy sediment including charcoal, fragments of tiles/bricks, blocks of slate shale as well as a batch of ceramic sherds mixing of Antiquity and Medieval (High Middle Ages? and Classical Middle Ages) elements. A full skeleton (fra008), belonging to a male aged >30 years, and other skeletal remains likely to come from three different individuals were buried in this site. Radiocarbon calibrated dating was retrieved under the scope of our study and indicates the skeleton dates to 943 - 1024 cal. AD.

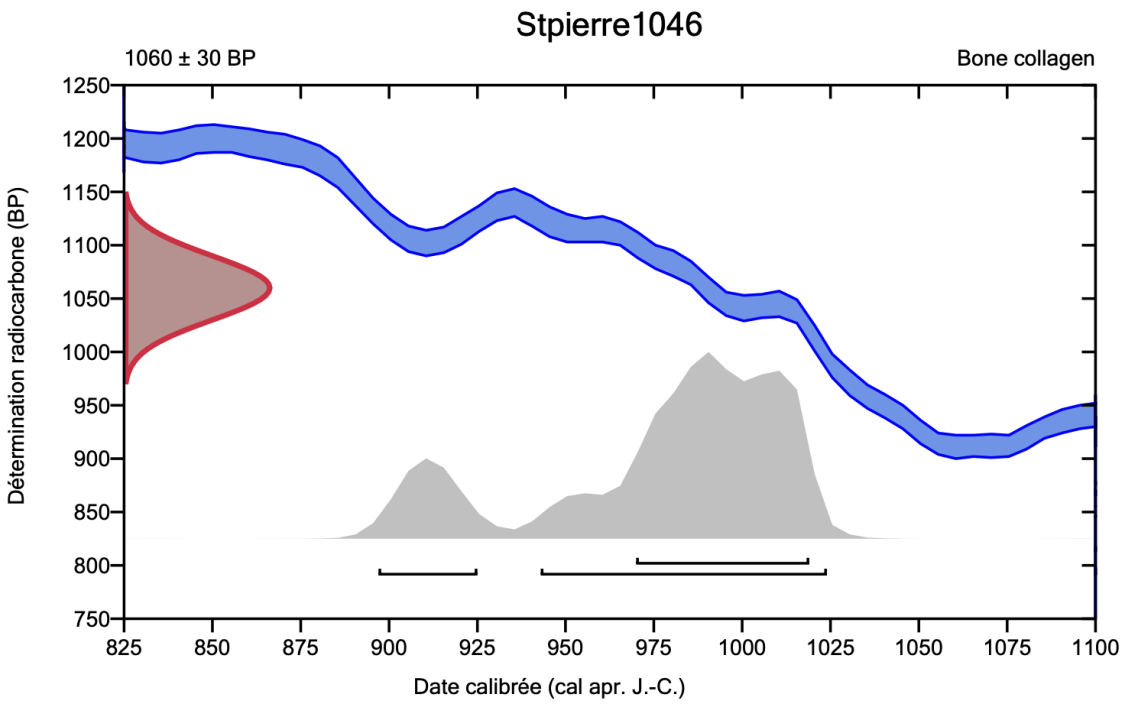

Figure S29: age graph of individual fra008 radiocarbon dating

Supplementary Discussion

1. Geolinguistics and genetic clusters

Below we describe in detail the overlap we found between dialectal areas and genetic clusters. However, these are not considered as biological relationships as they might reflect long-term inertia and socio-economic complex and cultural factors. Below the linguistic data come from the *Nouvel Atlas Linguistique de Basse-Bretagne* (1) and the places' names are extracted from the IGN BDtopo® database. A deeper understanding of such overlaps requires a higher resolution with respect to the genetic data.

1.1. Cluster "Bretagne-Centre", cluster "Cornouaille" and cluster "Vannes" together

The cluster "Bretagne-Centre" overlaps with the dialectal area featured by the usage of two initial consonants: the aspirated [h] instead of an unaspirated and the alveolar fricative [z] instead of [s], stretching respectively from the northern coast to the southern sea-side of the central area (Fig. S12). The river Blavet overlaps with the south-eastern boundaries of the dialectal areas and it separates, to some extent, the cluster "Bretagne-Centre" from the cluster "Vannes" (Fig. S14).
Fig. S12 'h-' shows seven analysed NALBB maps considering the treatment of the initial [h]. Fig. S12 'z-' represents the area where the initial [s] is voiced as [z]. The [z] area extends in a central crossing zone from the North to the South. It gradually disappears towards the southwest[1].
These two phonological features extend over an area between the southern coast of Morbihan and the north of the Côtes-d'Armor, excluding a north-western and a south-eastern area without the initial [h] and where the initial [s] is pronounced. Such phonological regions match with the distribution of "Bretagne-Centre" and "Cornouaille" clusters. The 'z-' map seems to correlate better than the 'h-' one. The articulation [z] for the initial [s] is also observed on the other side of the Channel, in the south-western dialects of England: *zome* 'some', *Zomerzet* 'Somerset', *to zwaip* for *to* sweep' fr. 'balayer', *zwell* for 'swell', *zwate* / *zweet* 'sweet' fr. 'doux' (Tristram 1995, Markus 2021). At this point, it would be interesting to compare the data from the People of the British Isles project (2,3) which shows a differentiation between the Cornwall and Devon clusters.

1.2. Cluster "Cornouaille"

If we would look for a coherence between the distribution of dialectal features in Lower-Brittany and "Cornouailles" cluster, we could consider the palatalization of *-h-* [h] into *-y-* [j] given their broad overlap (Fig. S13). This phenomenon can be found in the following words: *meryed* "girls", *luyadenn* "lightning", *luyed* "lightnings" and *meryer / dimeryer* 'Wednesday (noun/adv)'.

[1] A first analysis of the initial [z], according to NALBB data, was carried out by François Falc'hun, 1981, *Perspectives nouvelles sur l'histoire de la langue bretonne,* Union Générale d'Editions, fig. 67 p. 204.

1.3. Clusters ‘Léon’, ‘Cornouaille’, ‘Bretagne-Centre’, ‘Vannes’ and ‘Guérande’ and the Celto-Romance limit in eastern Brittany

All together the clusters “Léon”, “Cornouaille”, “Bretagne-Centre”, “Vannes” and “Guérande” correlate with the Celto-Romance limit attested between the 16th and the 18th centuries. The distribution of place-names Ker- attests the progressive withdrawal towards the west of this eastern limit of Celtic dialects (Fig. S26). According to Bernard Tanguy, the oriental limit of toponyms Ker- (Fig. S30) does not show the maximum extension of Breton spoken varieties but testifies the retreat of Armorican Gaulish dialects facing the gradual advance of the Gallo-Romance dialects in formation during the Early Middle Ages (4). The same toponymic element can be found on both sides of the Channel spelled *Ker-*, *Car-*, *Gear* in Cornwall (Joanne Pye 2019), and *Caer* in Wales (National Library of Wales 2021), Great Britain. So far, there is no evidence that the presence of *Ker-* place names in Brittany is due to a migration from Great Britain. If one considers the density of place-names as indicating a point of departure, it would indicate the opposite. At this stage it is more cautious to simply consider this toponymic element as a celtic linguistic and cultural mark.

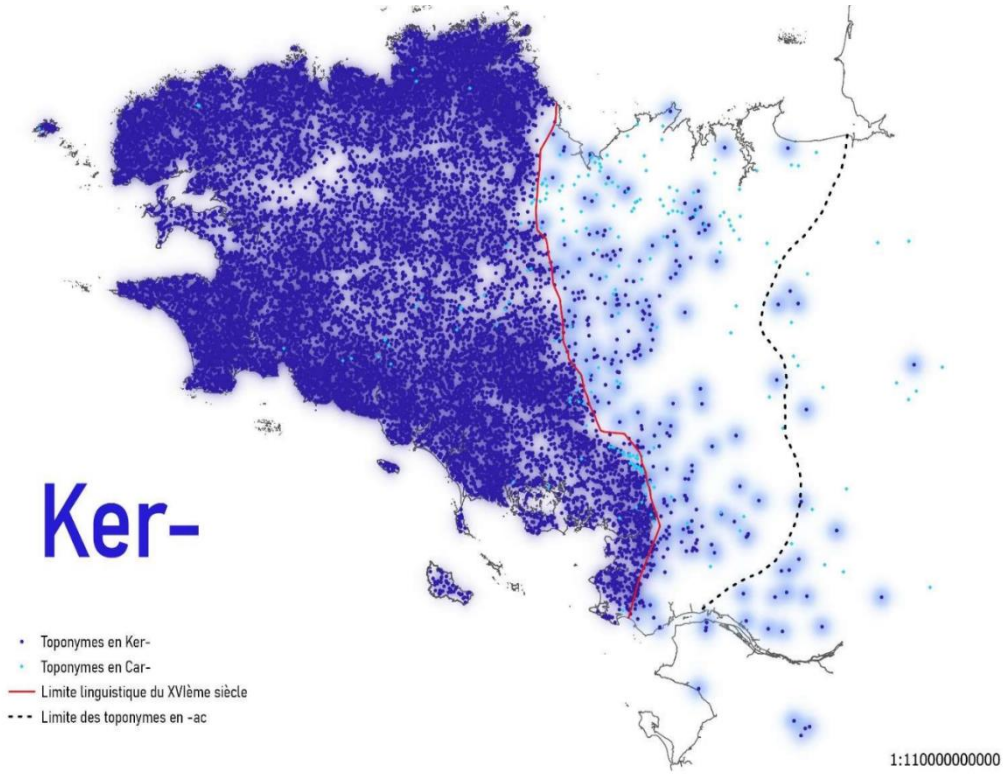

Figure S30. Distribution of *Ker-* “inhabited place”. Data : BDtopo®, National Geographic Institute (IGN). *Ker-* (royal blue) and *Car-* (turquoise) toponyms.

2. The role of rivers in the distribution of the 18 clusters

Rivers and streams could play a role in the diffusion of linguistic features. In France, the Loire initially formed an important border between the Oïl Gallo-Romance dialects in the North, and the Oc Gallo-Romance dialects in the South. Later, it became a vector for the diffusion of new traits coming from the North to the inner country (5). In Lower Brittany, on a smaller scale, the river Blavet seems to be at the origin of a bundle of isophones separating the different

treatments of the interdental spirants (6). The linguistic frontier separating the Celtic and Gallo-Romance areas is not determined by a natural barrier. Nevertheless, the hydrography seems to mark the territories within these zones. By using a geographical information system and the file of the main rivers proposed by the IGN's BDcarthage®, we assessed their role in the organisation of the k=18 genetic clusters.
We first discuss the rivers which seem to correspond to the limits of the genetic clusters. Cluster “Léon " is bordered in the north-east by the River of Morlaix and the Jarlot. In the South, the same cluster is separated from cluster “Cornouaille” by the river Aulne. The Laïta, extended by the Ellé until the north of Le Faouët, seems to border the cluster “Cornouaille”. The Carnoët forest could have reinforced its natural limit in the South. Cluster “Vannes” is enclosed on its western side by the Blavet and on its north side by the Oust. Cluster “Nantes” is circumscribed by the Semnon in the north and the Vilaine in the west. Cluster “Malo-Rennais” is surrounded by the Gouessant, then by the Yvel and the Hivet in the west, by the Canut and the Semnon further south. Finally, the Loire delimits the clusters “Guérande”, “Nantes” and “Ancenis” in the north and the clusters “Retz”, “Mauges 3” and “Mauges 1” in the south. In South Loire Vendée, we observe a role in the cluster landscape for rivers like “Le Lay” and “Sèvre Nantaise”, although it appears to be less clear. The “Maine-Anjou” cluster is crossed by several rivers and, when focusing at a finer, 78 clusters, scale, we also observe structuration along rivers like Mayenne, Vègre and Loir (data not shown).
The difference between navigable and non-navigable waterways does not seem to be decisive when considering the role of rivers by hampering gene flow. However, it has to be taken into account when studying their role as vectors. The geographical distribution of “Maine-Anjou'' includes the rivers Loire, Sarthe, Mayenne and Oudon, all of them are navigable waterways according to the *Service d'administration nationale des données et référentiels sur l'eau* (Sandre and IGN 2017). The cluster “Guérande” seems to be contained by the Vilaine mainly, the Oust, the Arz and the Brivet in the south. When we consider river geography, the distribution of clusters seems to be more complex than a simple cluster/bishoprics correlation.

3. Computer simulations to access the power to detect a short bottleneck with IBDNe

Identity-by-descent (IBD) sharing in population samples can be used to estimate recent effective population size changes. IBDNe (7) assumes an idealised random mating population with a constant effective size that has similar random changes in allele frequencies over time. Shorter IBD segments represent coalescent events that occurred further back in time, while longer segments represent coalescent events that occurred in the past few generations. If the number of IBD segments is high, a larger number of coalescent events have occurred, indicating a high coalescence probability meaning a low effective size. Similarly, if the number of IBD segments is low, the effective size is high.

The effective population size trajectories inferred in this study for the three main genetic clusters inferred with fineSTRUCTURE indicate a slight and short population decline, starting around the years 1,230-1,350 CE (13 generations and assuming a generation time ~29 year/generation) and lasting for almost ~300 years (~10 generations). Given the assumption of random mating within samples and our knowledge of extensive fine-scale structure within Northwestern France, this motivated us to perform a simulation study to assess whether a bottleneck could be detected if the evolutionary history of the population involves other scenarios other than a bottleneck.
More specifically, we investigated: 1) The performance of IBDNe in detecting a recent

bottleneck; 2) The effect of having admixture (punctual migration), sample structure and exponential growth in the estimation.
We used ARGON (8), a discrete time Wright-Fisher model simulator. Data was simulated for 50 diploid individuals (per population) according to a model containing 2 populations (see below). The data was simulated for each chromosome according to its respective size and we used the human recombination map (1000Genomes project). We ran the IBDNe software on our data using only IBD segments greater than 4cM. Simulated scenarios are shown below (Fig. S31).

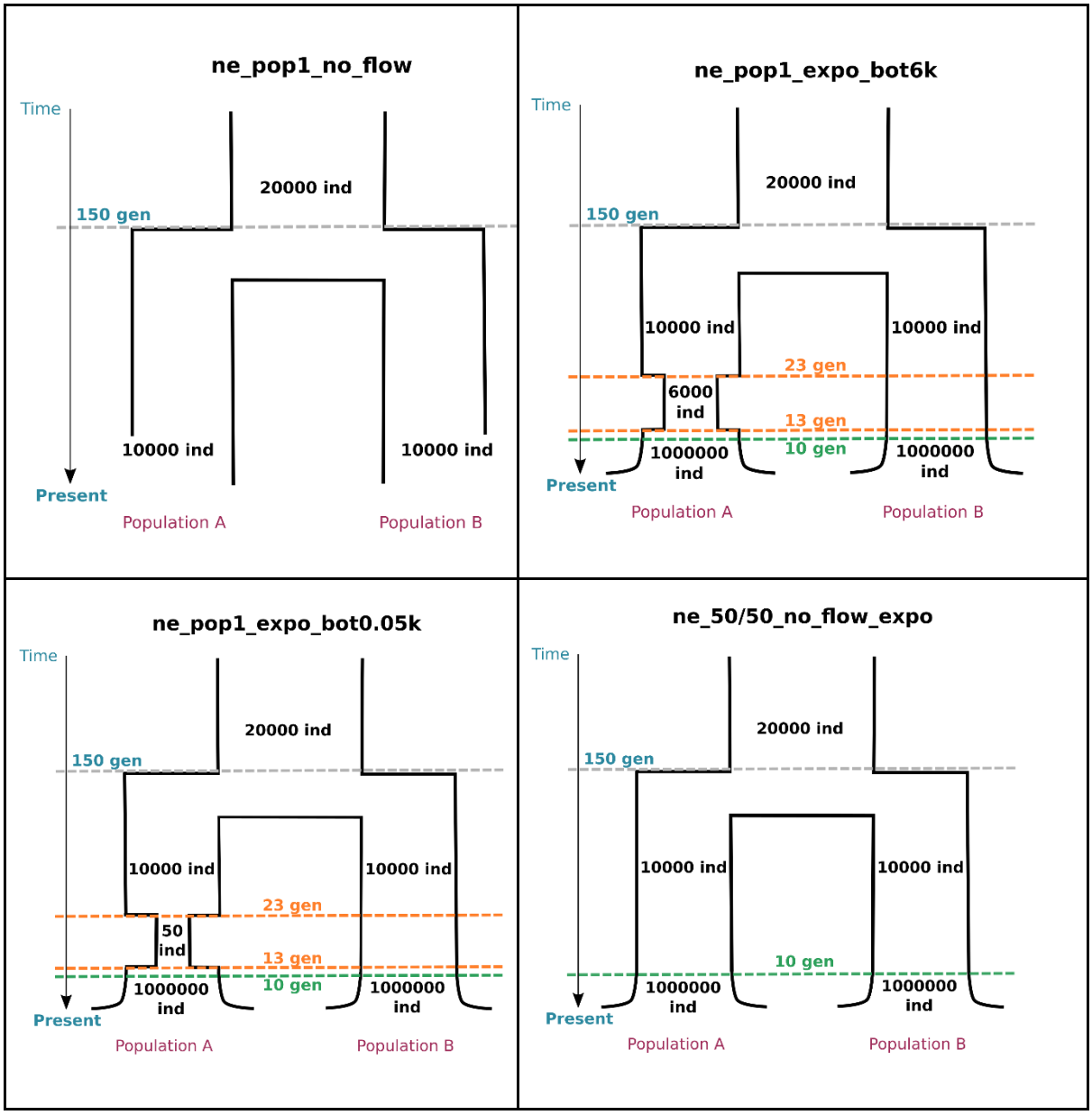

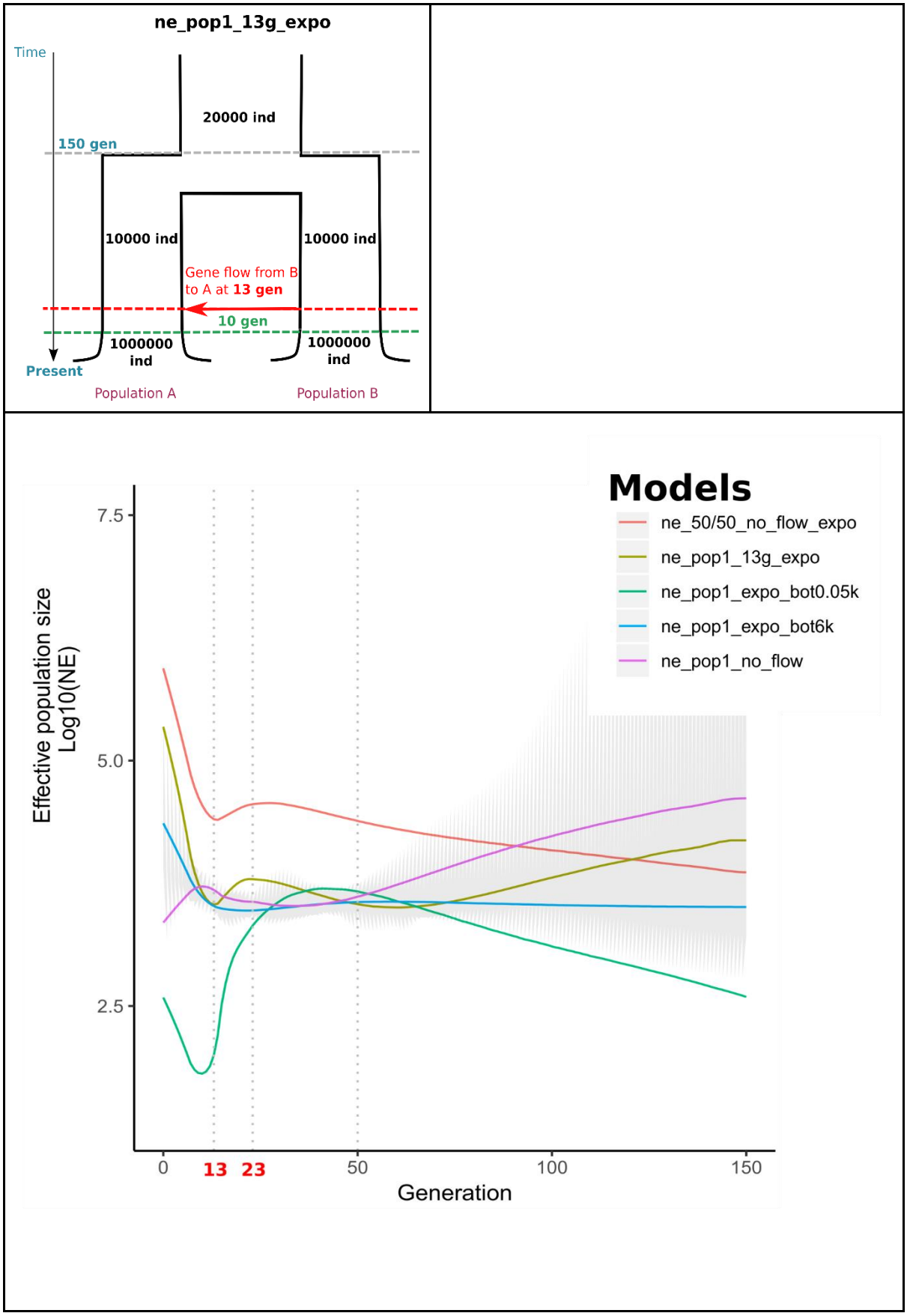

Figure S31. Simulation study performed to assess the power of IBDNe to infer short-lasting bottlenecks. We simulated models involving two populations that diverged 150

generations ago. Ne trajectories were inferred with IBDNe only from Population 1. The upper left panel represents the simplest model, in which after divergence Population 1 and 2 kept constant *Ne*. ne_pop1_expo_bot6k and ne_pop1_expo_bot0.05k models are variations of the simplest model, in which Population 1 undergoes 10 generations a long bottleneck after diverging from Population 2. Bottleneck starting times were set to 23 generations and the reduction in *Ne* were set to 6000/10000 and 50/10000, respectively. In model ne_50/50_no_flow_expo, Population 1 did not suffer a reduction in *Ne* but the sample analysed with IBDNe resulted from randomly sampling 50 individuals from both Population 1 and 2 in order to mimic population structure within the sample. Finally, the model ne_pop1_13g_flow_expo does not include a bottleneck but rather a one-generation event of gene flow. According to this model at generation 13 Population 1 has 10% of its lineages going to Population 2 (backwards in time). All models but the simplest one (upper left panel) include exponential growth in the last 10 generations as previously inferred in European populations (7,9).

We see that both the presence of stratification within the analysed sample represented here by the model ne_50/50_no_flow_expo (coral, Fig. S31) and the presence of admixture at generation 13 represented here by the model ne_pop1_13g_expo (kakhi, Fig. S31) induces a signal of a slight bottleneck similar to that found in the real dataset, with the drop in Ne and its recovery takes place in ~10 generations. In the case of an actual bottleneck, with a severe bottleneck represented here by the model ne_pop1_expo_bot0.05k (green colour, Fig. S31) and the bottleneck model (ne_pop1_expo_bot6k, turquoise colour, Fig. S31) with a reduction in size of ~⅓ of the original Ne, which is thought to have occurred during the black death period, we see that the actual start of the bottleneck is offset compared to the real timeframe (starting 23 generations ago). Therefore, we caution that short-lasting bottleneck signals from IBDNe trajectories may represent population structure or recent gene flow rather than a real bottleneck, which are inferred to exhibit a more progressive decrease and recovery than the reality.

4. References “merged ancient dataset”

The “merged ancient dataset” contains a subset of ancient (10–83) (84–90) and present-day samples (91–93) from the Allen Ancient DNA Resource (AADR) available in: https://reich.hms.harvard.edu/allen-ancient-dna-resource-aadr-downloadable-genotypes-present-day-and-ancient-dna-data. To the ancient samples we also added a set of ancient Vikings (94).

Supplementary References

1. Le Dû J. Nouvel atlas linguistique de la Basse-Bretagne. [Internet]. Brest: Centre de Recherche Bretonne et Celtique, Universite de Bretagne Occidentale; 2001. Available from: https://nouveau.univ-brest.fr/crbc/fr/page/nouvel-atlas-linguistique-de-basse-bretagne-en-ligne-nalbb-jean-le-du
2. Leslie S, Winney B, Hellenthal G, Davison D, Boumertit A, Day T, et al. The fine-scale genetic structure of the British population. Nature. 2015 Mar 19;519(7543):309–14.
3. Gilbert E, O’Reilly S, Merrigan M, McGettigan D, Molloy AM, Brody LC, et al. The Irish DNA Atlas: Revealing Fine-Scale Population Structure and History within Ireland. Sci Rep. 2017 08;7(1):17199.

4. Tanguy B. La limite linguistique dans la péninsule armoricaine à l'époque de l'émigration bretonne (IVe-Ve siècle) d'après les données toponymiques. Ann Bretagne Pays Ouest. 1980;87(3):429–62.
5. Brun-Trigaud G, Le Dû J, Le Berre Y. Lectures de l'Atlas Linguistique de la France de J. Gilléron et E. Edmont. Du temps dans l'espace [Internet]. CTHS; 2005 [cited 2022 Jan 31]. Available from: https://hal.archives-ouvertes.fr/hal-01360713
6. Falc'hun F. Méthode pour vérifier expérimentalement le sens de certains noms de lieux d'origine gauloise. Actes Colloq Société Fr Onomast. 1981;2(1):53–4.
7. Browning SR, Browning BL. Accurate Non-parametric Estimation of Recent Effective Population Size from Segments of Identity by Descent. Am J Hum Genet. 2015 Sep 3;97(3):404–18.
8. Palamara PF. ARGON: fast, whole-genome simulation of the discrete time Wright-fisher process. Bioinformatics. 2016 outubro;32(19):3032–4.
9. Athanasiadis G, Cheng JY, Vilhjálmsson BJ, Jørgensen FG, Als TD, Le Hellard S, et al. Nationwide Genomic Study in Denmark Reveals Remarkable Population Homogeneity. Genetics. 2016 Oct;204(2):711–22.
10. Raghavan M, Steinrücken M, Harris K, Schiffels S, Rasmussen S, DeGiorgio M, et al. Genomic evidence for the Pleistocene and recent population history of Native Americans. Science. 2015 Aug 21;349(6250):aab3884.
11. Saag L, Varul L, Scheib CL, Stenderup J, Allentoft ME, Saag L, et al. Extensive Farming in Estonia Started through a Sex-Biased Migration from the Steppe. Curr Biol. 2017 Jul;27(14):2185-2193.e6.
12. Saag L, Laneman M, Varul L, Malve M, Valk H, Razzak MA, et al. The Arrival of Siberian Ancestry Connecting the Eastern Baltic to Uralic Speakers further East. Curr Biol. 2019 May 20;29(10):1701-1711.e16.
13. Sánchez-Quinto F, Malmström H, Fraser M, Girdland-Flink L, Svensson EM, Simões LG, et al. Megalithic tombs in western and northern Neolithic Europe were linked to a kindred society. Proc Natl Acad Sci. 2019 May 7;116(19):9469–74.
14. Schiffels S, Haak W, Paajanen P, Llamas B, Popescu E, Loe L, et al. Iron Age and Anglo-Saxon genomes from East England reveal British migration history. Nat Commun. 2016 Jan 19;7(1):1–9.
15. Schroeder H, Margaryan A, Szmyt M, Theulot B, Włodarczak P, Rasmussen S, et al. Unraveling ancestry, kinship, and violence in a Late Neolithic mass grave. Proc Natl Acad Sci. 2019 May 28;116(22):10705–10.
16. Seguin-Orlando A, Korneliussen TS, Sikora M, Malaspinas AS, Manica A, Moltke I, et al. Genomic structure in Europeans dating back at least 36,200 years. Science. 2014 Nov 28;346(6213):1113–8.
17. Shinde V, Narasimhan VM, Rohland N, Mallick S, Mah M, Lipson M, et al. An Ancient Harappan Genome Lacks Ancestry from Steppe Pastoralists or Iranian Farmers. Cell. 2019 Oct;179(3):729-735.e10.
18. Sikora M, Seguin-Orlando A, Sousa VC, Albrechtsen A, Korneliussen T, Ko A, et al. Ancient genomes show social and reproductive behavior of early Upper Paleolithic foragers. Science. 2017 Nov 3;358(6363):659–62.
19. Sikora M, Pitulko VV, Sousa VC, Allentoft ME, Vinner L, Rasmussen S, et al. The population history of northeastern Siberia since the Pleistocene. Nature. 2019 Jun;570(7760):182–8.

20. Skoglund P, Malmström H, Omrak A, Raghavan M, Valdiosera C, Günther T, et al. Genomic Diversity and Admixture Differs for Stone-Age Scandinavian Foragers and Farmers. Science. 2014 May;344(6185):747–50.
21. de Barros Damgaard P, Martiniano R, Kamm J, Moreno-Mayar JV, Kroonen G, Peyrot M, et al. The first horse herders and the impact of early Bronze Age steppe expansions into Asia. Science. 2018 Jun 29;360(6396):eaar7711.
22. Allentoft ME, Sikora M, Sjögren KG, Rasmussen S, Rasmussen M, Stenderup J, et al. Population genomics of Bronze Age Eurasia. Nature. 2015 Jun;522(7555):167.
23. Amorim CEG, Vai S, Posth C, Modi A, Koncz I, Hakenbeck S, et al. Understanding 6th-century barbarian social organization and migration through paleogenomics. Nat Commun. 2018 Dec;9(1):3547.
24. Antonio ML, Gao Z, Moots HM, Lucci M, Candilio F, Sawyer S, et al. Ancient Rome: A genetic crossroads of Europe and the Mediterranean. Science. 2019 Nov 8;366(6466):708–14.
25. Brace S, Diekmann Y, Booth TJ, van Dorp L, Faltyskova Z, Rohland N, et al. Ancient genomes indicate population replacement in Early Neolithic Britain. Nat Ecol Evol [Internet]. 2019 Apr 15; Available from: https://doi.org/10.1038/s41559-019-0871-9
26. Brace S, Diekmann Y, Booth TJ, Dorp L van, Faltyskova Z, Rohland N, et al. Ancient genomes indicate population replacement in Early Neolithic Britain. Nat Ecol Evol. 2019 Apr 15;1.
27. Broushaki F, Thomas MG, Link V, López S, van Dorp L, Kirsanow K, et al. Early Neolithic genomes from the eastern Fertile Crescent. Science. 2016 Jul 29;353(6298):499–503.
28. Cassidy LM, Martiniano R, Murphy EM, Teasdale MD, Mallory J, Hartwell B, et al. Neolithic and Bronze Age migration to Ireland and establishment of the insular Atlantic genome. Proc Natl Acad Sci U S A. 2016 Jan 12;113(2):368–73.
29. Damgaard P de B, Marchi N, Rasmussen S, Peyrot M, Renaud G, Korneliussen T, et al. 137 ancient human genomes from across the Eurasian steppes. Nature. 2018 May;557(7705):369–74.
30. Fu Q, Hajdinjak M, Moldovan OT, Constantin S, Mallick S, Skoglund P, et al. An early modern human from Romania with a recent Neanderthal ancestor. Nature. 2015 Aug;524(7564):216–9.
31. Gamba C, Jones ER, Teasdale MD, McLaughlin RL, Gonzalez-Fortes G, Mattiangeli V, et al. Genome flux and stasis in a five millennium transect of European prehistory. Nat Commun [Internet]. 2014 Dec [cited 2019 Mar 15];5(1). Available from: http://www.nature.com/articles/ncomms6257
32. González-Fortes G, Jones ER, Lightfoot E, Bonsall C, Lazar C, Grandal-d'Anglade A, et al. Paleogenomic Evidence for Multi-generational Mixing between Neolithic Farmers and Mesolithic Hunter-Gatherers in the Lower Danube Basin. Curr Biol. 2017 Jun 19;27(12):1801-1810.e10.
33. González-Fortes G, Tassi F, Trucchi E, Henneberger K, Paijmans JLA, Díez-del-Molino D, et al. A western route of prehistoric human migration from Africa into the Iberian Peninsula. Proc R Soc B Biol Sci. 2019 Jan 23;286(1895):20182288.
34. Günther T, Malmström H, Svensson EM, Omrak A, Sánchez-Quinto F, Kılınç GM, et al. Population genomics of Mesolithic Scandinavia: Investigating early postglacial migration routes and high-latitude adaptation. PLOS Biol. 2018 Jan 9;16(1):e2003703.

35. Günther T, Valdiosera C, Malmström H, Ureña I, Rodriguez-Varela R, Sverrisdóttir ÓO, et al. Ancient genomes link early farmers from Atapuerca in Spain to modern-day Basques. Proc Natl Acad Sci. 2015 Sep;112(38):11917–22.
36. Haber M, Doumet-Serhal C, Scheib C, Xue Y, Danecek P, Mezzavilla M, et al. Continuity and Admixture in the Last Five Millennia of Levantine History from Ancient Canaanite and Present-Day Lebanese Genome Sequences. Am J Hum Genet. 2017 Aug;101(2):274–82.
37. Haber M, Doumet-Serhal C, Scheib CL, Xue Y, Mikulski R, Martiniano R, et al. A Transient Pulse of Genetic Admixture from the Crusaders in the Near East Identified from Ancient Genome Sequences. Am J Hum Genet. 2019 May;104(5):977–84.
38. Hajdinjak M, Fu Q, Hübner A, Petr M, Mafessoni F, Grote S, et al. Reconstructing the genetic history of late Neanderthals. Nature. 2018 Mar;555(7698):652–6.
39. Harney É, May H, Shalem D, Rohland N, Mallick S, Lazaridis I, et al. Ancient DNA from Chalcolithic Israel reveals the role of population mixture in cultural transformation. Nat Commun [Internet]. 2018 Dec [cited 2019 Feb 13];9(1). Available from: http://www.nature.com/articles/s41467-018-05649-9
40. Harney É, Nayak A, Patterson N, Joglekar P, Mushrif-Tripathy V, Mallick S, et al. Ancient DNA from the skeletons of Roopkund Lake reveals Mediterranean migrants in India. Nat Commun. 2019 Aug 20;10(1):3670.
41. Hofmanová Z, Kreutzer S, Hellenthal G, Sell C, Diekmann Y, Díez-del-Molino D, et al. Early farmers from across Europe directly descended from Neolithic Aegeans. Proc Natl Acad Sci. 2016 Jun;113(25):6886–91.
42. Järve M, Saag L, Scheib CL, Pathak AK, Montinaro F, Pagani L, et al. Shifts in the Genetic Landscape of the Western Eurasian Steppe Associated with the Beginning and End of the Scythian Dominance. Curr Biol. 2019 Jul;29(14):2430-2441.e10.
43. Jeong C, Balanovsky O, Lukianova E, Kahbatkyzy N, Flegontov P, Zaporozhchenko V, et al. The genetic history of admixture across inner Eurasia. Nat Ecol Evol. 2019 Jun;3(6):966–76.
44. Jeong C, Ozga AT, Witonsky DB, Malmström H, Edlund H, Hofman CA, et al. Long-term genetic stability and a high-altitude East Asian origin for the peoples of the high valleys of the Himalayan arc. Proc Natl Acad Sci. 2016 Jul 5;113(27):7485–90.
45. Jeong C, Wilkin S, Amgalantugs T, Bouwman AS, Taylor WTT, Hagan RW, et al. Bronze Age population dynamics and the rise of dairy pastoralism on the eastern Eurasian steppe. Proc Natl Acad Sci. 2018 Nov 27;115(48):E11248–55.
46. Jones ER, Zarina G, Moiseyev V, Lightfoot E, Nigst PR, Manica A, et al. The Neolithic Transition in the Baltic Was Not Driven by Admixture with Early European Farmers. Curr Biol. 2017 Feb;27(4):576–82.
47. Jones ER, Gonzalez-Fortes G, Connell S, Siska V, Eriksson A, Martiniano R, et al. Upper Palaeolithic genomes reveal deep roots of modern Eurasians. Nat Commun. 2015 Nov 16;6:8912.
48. Keller A, Graefen A, Ball M, Matzas M, Boisguerin V, Maixner F, et al. New insights into the Tyrolean Iceman's origin and phenotype as inferred by whole-genome sequencing. Nat Commun. 2012 Feb;3:698.
49. Kılınç GM, Omrak A, Özer F, Günther T, Büyükkarakaya AM, Bıçakçı E, et al. The Demographic Development of the First Farmers in Anatolia. Curr Biol. 2016 Oct;26(19):2659–66.

50. Krzewińska M, Kjellström A, Günther T, Hedenstierna-Jonson C, Zachrisson T, Omrak A, et al. Genomic and Strontium Isotope Variation Reveal Immigration Patterns in a Viking Age Town. Curr Biol. 2018 Sep 10;28(17):2730-2738.e10.
51. Krzewińska M, Kılınç GM, Juras A, Koptekin D, Chyleński M, Nikitin AG, et al. Ancient genomes suggest the eastern Pontic-Caspian steppe as the source of western Iron Age nomads. Sci Adv. 4(10):eaat4457.
52. Lamnidis TC, Majander K, Jeong C, Salmela E, Wessman A, Moiseyev V, et al. Ancient Fennoscandian genomes reveal origin and spread of Siberian ancestry in Europe. Nat Commun. 2018 Nov 27;9(1):5018.
53. Lazaridis I, Patterson N, Mittnik A, Renaud G, Mallick S, Kirsanow K, et al. Ancient human genomes suggest three ancestral populations for present-day Europeans. Nature. 2014 Sep 18;513(7518):409–13.
54. Lazaridis I, Nadel D, Rollefson G, Merrett DC, Rohland N, Mallick S, et al. Genomic insights into the origin of farming in the ancient Near East. Nature. 2016 Aug;536(7617):419–24.
55. Lazaridis I, Mittnik A, Patterson N, Mallick S, Rohland N, Pfrengle S, et al. Genetic origins of the Minoans and Mycenaeans. Nature. 2017 Aug;548(7666):214.
56. Lipson M, Skoglund P, Spriggs M, Valentin F, Bedford S, Shing R, et al. Population Turnover in Remote Oceania Shortly after Initial Settlement. Curr Biol. 2018 Apr;28(7):1157-1165.e7.
57. Lipson M, Szécsényi-Nagy A, Mallick S, Pósa A, Stégmár B, Keerl V, et al. Parallel palaeogenomic transects reveal complex genetic history of early European farmers. Nature. 2017 Nov;551(7680):368–72.
58. Lipson M, Ribot I, Mallick S, Rohland N, Olalde I, Adamski N, et al. Ancient West African foragers in the context of African population history. Nature. 2020 Jan;577(7792):665–70.
59. Lipson M, Cheronet O, Mallick S, Rohland N, Oxenham M, Pietrusewsky M, et al. Ancient genomes document multiple waves of migration in Southeast Asian prehistory. Science. 2018 Jul 6;361(6397):92–5.
60. Llorente MG, Jones ER, Eriksson A, Siska V, Arthur KW, Arthur JW, et al. Ancient Ethiopian genome reveals extensive Eurasian admixture in Eastern Africa. Science. 2015 Nov;350(6262):820–2.
61. Malmström H, Günther T, Svensson EM, Juras A, Fraser M, Munters AR, et al. The genomic ancestry of the Scandinavian Battle Axe Culture people and their relation to the broader Corded Ware horizon. Proc R Soc B Biol Sci. 2019 Oct 9;286(1912):20191528.
62. Martiniano R, Caffell A, Holst M, Hunter-Mann K, Montgomery J, Müldner G, et al. Genomic signals of migration and continuity in Britain before the Anglo-Saxons. Nat Commun. 2016 Jan 19;7:10326.
63. Martiniano R, Cassidy LM, Ó'Maoldúin R, McLaughlin R, Silva NM, Manco L, et al. The population genomics of archaeological transition in west Iberia: Investigation of ancient substructure using imputation and haplotype-based methods. PLOS Genet. 2017 Jul 27;13(7):e1006852.
64. Mathieson I, Lazaridis I, Rohland N, Mallick S, Patterson N, Roodenberg SA, et al. Genome-wide patterns of selection in 230 ancient Eurasians. Nature. 2015 Dec 24;528(7583):499–503.
65. Mathieson I, Alpaslan-Roodenberg S, Posth C, Szécsényi-Nagy A, Rohland N, Mallick S, et al. The genomic history of southeastern Europe. Nature. 2018 Feb 21;555(7695):197–203.

66. Meyer M, Kircher M, Gansauge MT, Li H, Racimo F, Mallick S, et al. A High-Coverage Genome Sequence from an Archaic Denisovan Individual. Science. 2012 Oct;338(6104):222–6.
67. Mittnik A, Wang CC, Pfrengle S, Daubaras M, Zariņa G, Hallgren F, et al. The genetic prehistory of the Baltic Sea region. Nat Commun. 2018 Jan 30;9(1):442.
68. Mittnik A, Massy K, Knipper C, Wittenborn F, Friedrich R, Pfrengle S, et al. Kinship-based social inequality in Bronze Age Europe. Science. 2019 Nov 8;366(6466):731–4.
69. Moreno-Mayar JV, Vinner L, Damgaard P de B, Fuente C de la, Chan J, Spence JP, et al. Early human dispersals within the Americas. Science. 2018 Dec 7;362(6419):eaav2621.
70. Narasimhan VM, Patterson N, Moorjani P, Rohland N, Bernardos R, Mallick S, et al. The formation of human populations in South and Central Asia. Science. 2019 Sep 6;365(6457):eaat7487.
71. Nikitin AG, Stadler P, Kotova N, Teschler-Nicola M, Price TD, Hoover J, et al. Interactions between earliest Linearbandkeramik farmers and central European hunter gatherers at the dawn of European Neolithization. Sci Rep. 2019 Dec 20;9(1):19544.
72. Ning C, Wang CC, Gao S, Yang Y, Zhang X, Wu X, et al. Ancient Genomes Reveal Yamnaya-Related Ancestry and a Potential Source of Indo-European Speakers in Iron Age Tianshan. Curr Biol. 2019 Aug 5;29(15):2526-2532.e4.
73. Olalde I, Brace S, Allentoft ME, Armit I, Kristiansen K, Booth T, et al. The Beaker phenomenon and the genomic transformation of northwest Europe. Nature. 2018 Mar 8;555(7695):190–6.
74. Olalde I, Mallick S, Patterson N, Rohland N, Villalba-Mouco V, Silva M, et al. The genomic history of the Iberian Peninsula over the past 8000 years. Science. 2019 Mar 15;363(6432):1230–4.
75. Olalde I, Allentoft ME, Sánchez-Quinto F, Santpere G, Chiang CWK, DeGiorgio M, et al. Derived immune and ancestral pigmentation alleles in a 7,000-year-old Mesolithic European. Nature. 2014 Mar;507(7491):225.
76. Olalde I, Schroeder H, Sandoval-Velasco M, Vinner L, Lobón I, Ramirez O, et al. A Common Genetic Origin for Early Farmers from Mediterranean Cardial and Central European LBK Cultures. Mol Biol Evol. 2015 Dec;32(12):3132–42.
77. Omrak A, Günther T, Valdiosera C, Svensson EM, Malmström H, Kiesewetter H, et al. Genomic Evidence Establishes Anatolia as the Source of the European Neolithic Gene Pool. Curr Biol. 2016 Jan;26(2):270–5.
78. Pickrell JK, Patterson N, Loh PR, Lipson M, Berger B, Stoneking M, et al. Ancient west Eurasian ancestry in southern and eastern Africa. Proc Natl Acad Sci. 2014 Feb 18;111(7):2632–7.
79. Prendergast ME, Lipson M, Sawchuk EA, Olalde I, Ogola CA, Rohland N, et al. Ancient DNA reveals a multistep spread of the first herders into sub-Saharan Africa. Science. 2019 Jul 5;365(6448):eaaw6275.
80. Prüfer K, De Filippo C, Grote S, Mafessoni F, Korlević P, Hajdinjak M, et al. A high-coverage Neandertal genome from Vindija Cave in Croatia. Science. 2017 Nov 3;358(6363):655–8.
81. Prüfer K, Racimo F, Patterson N, Jay F, Sankararaman S, Sawyer S, et al. The complete genome sequence of a Neanderthal from the Altai Mountains. Nature. 2014 Jan;505(7481):43–9.

82. Raghavan M, Skoglund P, Graf KE, Metspalu M, Albrechtsen A, Moltke I, et al. Upper Palaeolithic Siberian genome reveals dual ancestry of Native Americans. Nature. 2014 Jan;505(7481):87–91.
83. Raghavan M, DeGiorgio M, Albrechtsen A, Moltke I, Skoglund P, Korneliussen TS, et al. The genetic prehistory of the New World Arctic. Science. 2014 Aug 29;345(6200):1255832.
84. Unterländer M, Palstra F, Lazaridis I, Pilipenko A, Hofmanová Z, Groß M, et al. Ancestry and demography and descendants of Iron Age nomads of the Eurasian Steppe. Nat Commun. 2017 Mar 3;8:14615.
85. Valdiosera C, Günther T, Vera-Rodríguez JC, Ureña I, Iriarte E, Rodríguez-Varela R, et al. Four millennia of Iberian biomolecular prehistory illustrate the impact of prehistoric migrations at the far end of Eurasia. Proc Natl Acad Sci. 2018 Mar 27;115(13):3428–33.
86. Veeramah KR, Rott A, Groß M, Dorp L van, López S, Kirsanow K, et al. Population genomic analysis of elongated skulls reveals extensive female-biased immigration in Early Medieval Bavaria. Proc Natl Acad Sci. 2018 Mar 27;115(13):3494–9.
87. Villalba-Mouco V, van de Loosdrecht MS, Posth C, Mora R, Martínez-Moreno J, Rojo-Guerra M, et al. Survival of Late Pleistocene Hunter-Gatherer Ancestry in the Iberian Peninsula. Curr Biol. 2019 Apr;29(7):1169-1177.e7.
88. Wang CC, Reinhold S, Kalmykov A, Wissgott A, Brandt G, Jeong C, et al. Ancient human genome-wide data from a 3000-year interval in the Caucasus corresponds with eco-geographic regions. Nat Commun. 2019 Feb 4;10(1):590.
89. Zalloua P, Collins CJ, Gosling A, Biagini SA, Costa B, Kardailsky O, et al. Ancient DNA of Phoenician remains indicates discontinuity in the settlement history of Ibiza. Sci Rep. 2018 Dec 4;8(1):17567.
90. van de Loosdrecht M, Bouzouggar A, Humphrey L, Posth C, Barton N, Aximu-Petri A, et al. Pleistocene North African genomes link Near Eastern and sub-Saharan African human populations. Science. 2018 May 4;360(6388):548–52.
91. The 1000 Genomes Project Consortium, Gibbs RA, Boerwinkle E, Doddapaneni H, Han Y, Korchina V, et al. A global reference for human genetic variation. Nature. 2015 Oct;526(7571):68–74.
92. Patterson N, Moorjani P, Luo Y, Mallick S, Rohland N, Zhan Y, et al. Ancient Admixture in Human History. Genetics. 2012 Nov 1;192(3):1065–93.
93. Mallick S, Li H, Lipson M, Mathieson I, Gymrek M, Racimo F, et al. The Simons Genome Diversity Project: 300 genomes from 142 diverse populations. Nature. 2016 Oct 13;538(7624):201–6.
94. Margaryan A, Lawson DJ, Sikora M, Racimo F, Rasmussen S, Moltke I, et al. Population genomics of the Viking world. Nature. 2020 Sep;585(7825):390–6.